



**International
Collaboration
Center**

Institute for Materials Research
Tohoku University

ICC-IMR FY2010 Activity Report

<http://www.icc-imr.imr.tohoku.ac.jp/>

ICC-IMR FY2010

Activity Report

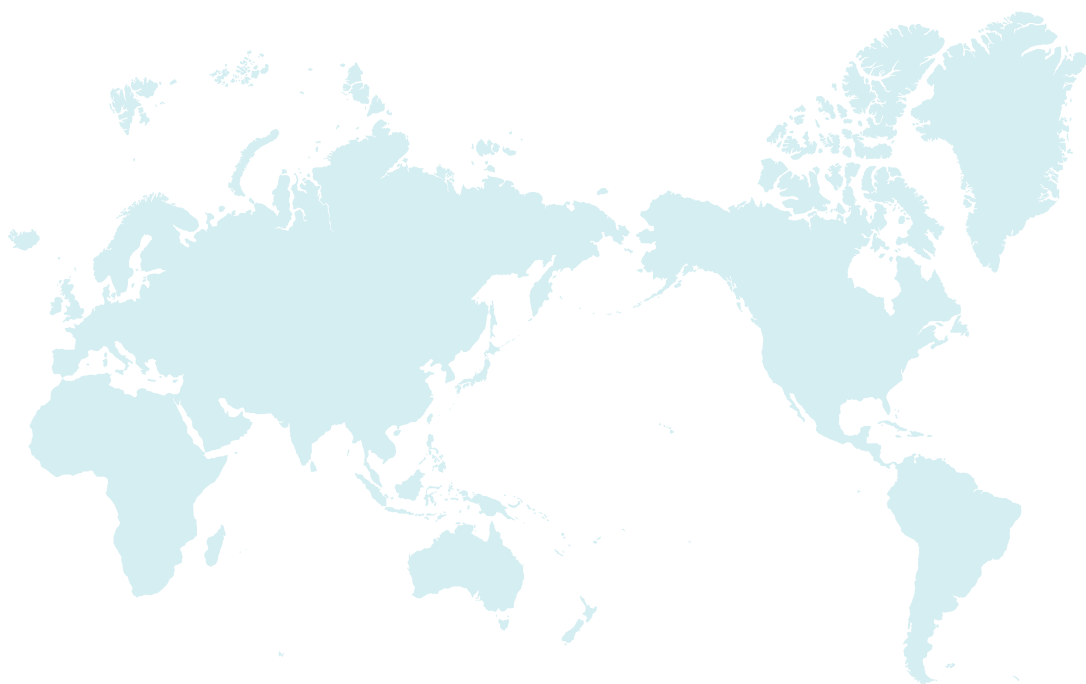
International Collaboration Center

Institute for Materials Research
Tohoku University

CONTENTS



Mission	02
Committee Members	03
Visiting Scholars	05
Workshops	17
KINKEN WAKATE	23
Short-term Visiting Researchers	27



Mission

The ICC-IMR was founded in April 2008 as the center for international collaboration of the Institute for Materials Research (IMR) a center of excellence in material science, consisting of 24 research groups and five research centers. The ICC-IMR works as a gateway of diverse collaborations between overseas and IMR researchers. The ICC-IMR has invited 18 visiting professors and conducted 9 international research projects since its start-up (please inspect the graph below for more details,). The applications are open to foreign researchers and the projects are evaluated by a peer-review process involving international reviewers.

ICC-IMR coordinates six different programs:

- 1) International Integrated Project Research
- 2) Visiting Professorships
- 3) Short Single Research Visits
- 4) International Workshops
- 5) Fellowship for Young Researcher and PhD Student
- 6) Material Transfer Program

We welcome applicants from around the globe to submit proposals!

ICC-IMR COMMITTEE MEMBERS

Director

Prof. Hiroyuki NOJIRI

Steering Committee

Prof. Takashi Goto

Prof. Koki Takanashi

Prof. Toyohiko Konno

Prof. Shin-ichi ORIMO

Prof. Eiji SAITOH

Assoc. Prof. Kenji Ohoyama

Activity Report

Visiting Scholars



FY 2010 Visiting Scholars

No.	Candidate	Host	Proposed Research	Title	Affiliation	Term
10G1	Hao Chen	Y. Kawazoe	Theoretical Study on Electron Transport	Professor	Fudan University, China	2010.6.15-9.14
10G2	Thierry Epicier	T. Konno	Materials Science, Structural Analysis by Using TEM	Professor	CNRS nad INSA de Lyon, France	2010.7.10-8.9
10G3	Arndt Remhof	S. Orimo	Lithium Fast-ionic Conductivity in Complex Hydrides	Group Leader	Empa Materials Science and Technology, Switzerland	2010.8.25-10.16
10G4	Baolong Shen	A. Makino	Fe-Based Nanocrystalline Soft-Magnetic Alloys with High Bs and High Curie Temperature	Professor	Ningbo Institute of Materials Technology and Engineering, Chinese Academy of Sciences, China	2010.10.1-12.31
10G5	Yu In-Keun	K. Watanabe	Feasibility Study of a Toroid-Type HTS SMES Application to Power Quality Enhancement Using Power-Hardware-in-the-Loop Simulation	Professor	Changwon National University, Korea	2010.10.1-12.31
10G6	Vargas Garcia Jorge Roberto	T. Goto	Ceria-Based Films Prepared by Laser CVD	Professor	National Polytechnic Institute, Mexico	2011.1.1-3.31

Hydrogenation-chain created conduction channels in zigzag graphene nanoribbons

We discover a method of opening the conductive channels of zigzag graphene nanoribbons (ZGNRs) by using hydrogenation chains to separate the nanoribbon into two strips with a $\sim 0.7 \text{ \AA}$ distance, although the overall hydrogenation on graphene transforms the highly conductive semimetal sheet into an insulator.

The zigzag graphene nanoribbons with edges, terminated by hydrogen atoms, have the strongly localized states (namely edge states) carrying conductive charges. The edge states corresponding to the partly flat band near Fermi energy have large contributions to the density of states. Nakada and coworkers [1] analytically derived the existence of edge states for ZGNRs. In the quantum Hall experiments, the current-carrying localized edge states in the Landau energy gap play an essential role in the Laughlin's gauge invariance argument [2].

We study the role of hydrogenation chains in the process of electronic transport in ZGNRs. In order to enhance the conduction of the graphene nanoribbons, we design modified nanoribbons with one or two carbon chains hydrogenated on opposite faces of the nanoribbon sheet. By elongating the carbon-carbon bonds, the graphane-like hydrogenation chain decreases the conduction ability of the carbon chain and forms a quasi-edge in the central region of the ribbon. On both sides of the hydrogenation carbon chain a new edge-like state appears and enhances the conduction ability of ZGNRs.

Before calculating the transport properties of nanoribbons, we optimize their configurations with B3LYP as exchange-correlation functional, and 6-31g as basis set, convergence on maximum and root-mean-square (RMS) density matrix (10^{-8}), max density matrix (10^{-6}), and energy (10^{-6}) Ry., respectively. The periodic boundary condition (PBC) optimization is done by using 100 k points with the initial structure parameters obtained from a large ZGNR cluster optimization calculation. The hydrogenated carbon atoms are out of the nanoribbon plane due to the bond extension. In Fig. 1, the side view (down pattern) of 7ZGNR2H shows the hydrogenated carbon atoms with distances in \AA perpendicular to the ribbon (from top to bottom: 0.43, -0.19, 0.19, and -0.43).

We demonstrate that the hydrogenation chains may have the different effect on conductance of zigzag graphene nanoribbons, although the hydrogenation ex-

tends the length of carbon-carbon bond in graphene, and transforms the highly conductive semimetal sheet into an insulator, namely graphane. The hydrogenation chains on ZGNRs open the new edge-like states and enhance the conductive abilities of the ZGNRs by separating the nanoribbon into several narrow strips separated by distance from 0.62 \AA (for 7ZGNR2H) to 0.70 \AA (for 7ZGNRH) \AA . Furthermore the hydrogenation chains drive the even-

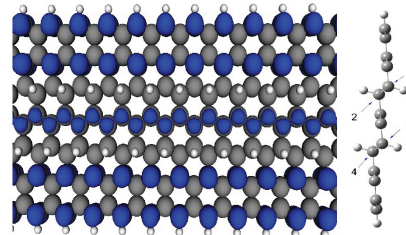


FIG. 1. Configuration and LDOS of 7ZGNR2H. The side view shows the three strips separated by two hydrogenation chains.

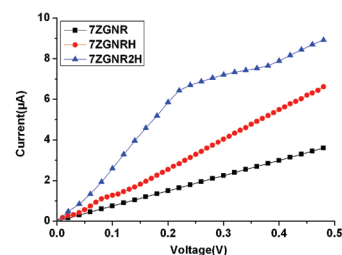


FIG. 2. Current of seven-chain zigzag graphene nanoribbons with/without hydrogenation chains.

row 6ZGNR from a poor conductive state to a metallic one. For 5ZGNRH, we obtain the results (not shown in the paper to avoid duplicate) similar to 7ZGNRH. The fact that each hydrogenation chain creates two conduction channels around itself, which enhances the conductance of ZGNRs, is valid for 5ZGNRH, 7ZGNRH, 7ZGNR2H, and 6ZGNRH. Our numerical calculations demonstrate a novel way for the hydrogenation chains of being used in the nanoelectronics and carbonelectronics engineering.

The work is done with D.D.Wu, F. Jiang, G. Yin, Y.Y. Liang, H. Mizuseki, and Y. Kawazoe.

- [1] K. Nakada, M. Fujita, G. Dresselhaus, and M.S. Dresselhaus, *Phy. Rev. B* **54**, 17954 (1996).
 [2] B.I. Halperin, *Phys. Rev. B* **25**, 2185 (1982).

Key Words

Edge state, Hydrogenation chain, Nanoribbon
Contact to
 Hao Chen (Physics Department, Fudan University, Shanghai, China)
 E-mail: haochen@fudan.edu.cn

DETECTION of RARE EARTH DOPANTS at the ATOMIC LEVEL in YAG-based OPTICAL CERAMICS

Optimizing specific properties of materials frequently involves the addition of small quantities of 'dopants', the detection of which may require an investigation at the atomic level. This is the case of optical, luminescent ceramics (such as YAG polycrystals) doped with rare earth elements. We demonstrate here the positive quantitative analysis of Yb dopants in such a YAG polycrystals by means of high resolution HAADF-STEM imaging in the TITAN, 300 kV transmission electron microscope of the IMR.

The research activity on advanced optical materials for various applications, such as lasers, scintillators, is greatly increasing with the availability of sintered polycrystalline ceramics. Understanding their optical properties requires a detailed investigation of their microstructure, especially regarding the exact location of the required dopants (e.g. rare earth elements such as Ce^{3+} , Nd^{3+} or Yb^{3+}). For example, it was recently shown by careful Transmission Electron Microscopy (TEM) observations that Ce strongly segregates at grain-boundaries within YAG (Yttrium Aluminium Garnet $Y_3Al_5O_{12}$) [1].

Identifying dopants at the atomic level by Electron Microscopy techniques is now possible according to the technological progress, especially in the so-called STEM-HAADF mode [2].

STEM-HAADF imaging (Scanning TEM in High Angle Annular Dark Field) consists in scanning the electron probe on the sample, and collecting on an annular detector the primary electrons scattered at high angle. In such a process, the scattered signal is roughly proportional to Z^2 , where Z is the atomic number of the probed species. Then, heavy atoms (such as rare-earth elements) give rise to a brighter contrast than lighter species (such as O, Al and even Y in the YAG structure). Atomic resolution is achieved if the probe size is smaller than the interatomic distance within the material of interest under some specific viewing crystallographic directions.

We have performed both High Resolution (HR) and HAADF imaging on pure YAG and Yb-doped YAG polycrystals, using a TITAN FEI electron microscope, operating at 300 kV. On the one hand, this instrument is equipped with a C_s aberration corrector on the objective lens, allowing a resolution down to 0.1 nm to be obtained in the HREM mode. On the other hand, it is also equipped with an annular detector collecting electrons in a 70-210 mRad angular range. Nanoprobe chemical analysis was also simultaneously performed using an EDAX EDX (Energy-Dispersive X-ray) analyser mounted on the microscope. Whereas C_s -corrected HREM failed to reveal the distribution of

Yb-containing atomic columns, the STEM-HAADF imaging mode appeared to be more efficient owing to its sensitivity to Z . Figure 1 shows a comparison of a 1.4 at.%Yb-doped and a pure YAG samples when observed along the [001] azimuth. A high density of brighter columns is observed for the doped material, which can be consistently analysed in terms of statistics as imaging Yb-containing atomic columns. Dedicated

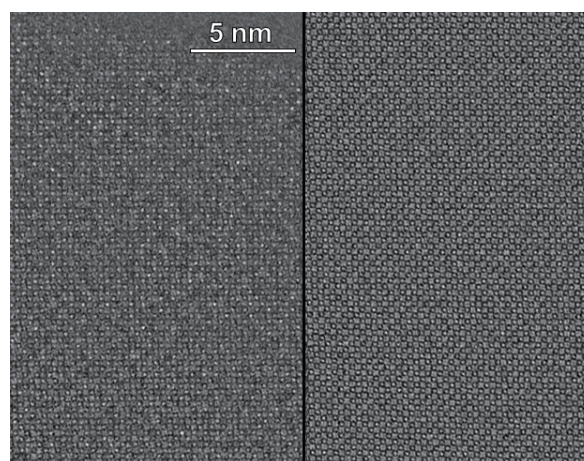


Fig. 1 HAADF-STEM images of two regions of similar thicknesses (as attested by low-loss EELS spectra) from a 1.4 at. % Yb-doped sample (left) and a pure YAG sample (right).

HAADF-STEM image simulations confirm this finding. This work shows that no segregation, neither clustering of Yb ions occurs in polycrystalline YAG.

References

- [1] ZHAO W., MANCINI C., AMANS D., BOULON G., EPICIER T., MIN Y., YAGI H., YANAGITANI T., YANAGIDA T., YOSHIKAWA A., *Jap. J. Appl. Physics* 49 (2010) 022602
- [2] VOYLES PM., GRAZUL JL., MULLER DA., *Ultramicrosc.* 96 (2003) 251.

Key Words

Optical ceramics, Yb-doped YAG, atomic STEM-HAADF

Contact to

Thierry EPICIER (MATEIS, INSA-Lyon, umr CNRS 5510, Bât. Blaise Pascal, 69621 Villeurbanne Cedex, FRANCE)

E-mail: thierry.epicier@insa-lyon.fr

<http://clym.insa-lyon.fr>

Lithium Fast-Ion Conduction in Complex Hydrides

A few years ago, an exceptional high Li mobility was discovered within the high temperature (HT) phase of LiBH_4 by IMR scientists [1]. Stabilizing the HT phase by adding lithium halides results in an enhanced conductivity at room temperature [2]. Even higher conductivities are reached by combining BH_4^- and NH_2^- anions in compounds such as $\text{Li}_2(\text{BH}_4)(\text{NH}_2)$ [3]. We investigated LiBH_4 based compounds in view of their potential applications as Li-ion conductors and/or as hydrogen storage materials

Continuous depletion of fossil fuels and growing environmental concerns make energy supply one of the major challenges in the 21st century. The implementation of renewable energy requires new high performance materials for energy conversion, transport and storage. For industrial applications these materials have to be cheap, safe and reliable in their performance. Currently, materials for lithium ion batteries, photovoltaics, fuel cells and electrolyser cells, and materials for hydrogen production and storage are in the focus of many research activities worldwide.

Borohydrides are ionic stable materials that contain light metal cation and BH_4^- groups, which are considered as high performance hydrogen storage media. Recently an exceptional high Li mobility was discovered within the high temperature (HT) phase of LiBH_4 . Stabilization of the HT phase of this compound by addition of lithium halides results in an enhanced conductivity also at room temperature. Even higher conductivities are reached by combining $(\text{BH}_4)^-$ and $(\text{NH}_2)^-$ anions in compounds such as $\text{Li}_2(\text{BH}_4)(\text{NH}_2)$, as shown in fig.1.

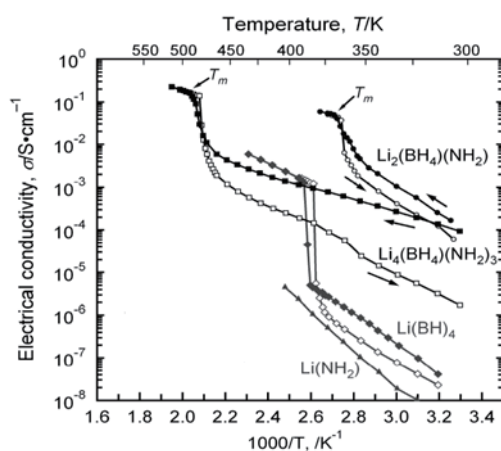


Figure 1: Electrical conductivities of LiBH_4 , LiNH_2 , $\text{Li}_2(\text{BH}_4)(\text{NH}_2)$ and $\text{Li}_4(\text{BH}_4)(\text{NH}_2)_3$ (triangle).

Up to now, the origin of the phase transition, and therefore the

role of the halides as stabilizing agents are not understood. Also the transport mechanism in borohydrides and the influence of the rapid localized motion of the $(\text{BH}_4)^-$ anion on the conductivity is not known so far, as well as hydrogen transport in general that is crucial for tuning materials' properties for purpose of the energy storage by means of hydrogen.

We investigated the hydrogen dynamics [4] and the electrical conductivity of pure LiBH_4 as well as of the LiBH_4 based complex hydrides $\text{Li}_2(\text{BH}_4)(\text{NH}_2)$ and $\text{Li}_4(\text{BH}_4)(\text{NH}_2)_3$ in the solid as well as in the liquid state [5]. The two $(\text{NH}_2)^-$ containing hydrides show lithium fast-ion conductivities of about 1×10^{-4} S/cm at room temperature. After melting, the total ion conductivities of $\text{Li}_2(\text{BH}_4)(\text{NH}_2)$ and $\text{Li}_4(\text{BH}_4)(\text{NH}_2)_3$ increase up to 6×10^{-2} S/cm (378 K) and 2×10^{-1} S/cm (513 K), respectively.

We also investigated the hydrogen release reactions of LiBH_4 . In the past, different routes were suggested and different intermediate products have been found experimentally. We could show that by carefully choosing parameters such as temperature and applied hydrogen pressure, the preferred decomposition route may be selected [6].

References

- [1] M. Matsuo, Y. Nakamori, S. Orimo, H. Maekawa and H. Takamura: Appl. Phys. Lett. **91** (2007) 224103.
- [2] H. Maekawa, M. Matsuo, H. Takamura, M. Ando, Y. Noda, T. Karahashi and S. Orimo: J. Am. Chem. Soc. **131** (2009) 894
- [3] M. Matsuo, A. Remhof, P. Martelli, R. Caputo, M. Ernst, Y. Miura, T. Sato, H. Oguchi, H. Maekawa, H. Takamura, A. Borgschulte, A. Züttel and S. Orimo: J. Am. Chem. Soc. **131** (2009) 16389
- [4] P. Martelli, A. Remhof, A. Züttel, S. I. Orimo, et al. in preparation.
- [5] Y. Zhou, M. Matsuo, Y. Miura, H. Takamura, H. Maekawa, A. Remhof, A. Borgschulte, A. Züttel, T. Otomo, S. Orimo, Mater. Trans., in press
- [6] Y. Yan, A. Remhof, H.W. Li, A. Züttel, S. Orimo, in preparation.

Key Words

Li-ion conductivity, hydrogen storage, impedance spectroscopy

Contact to

Arndt Remhof, Empa – Swiss Federal Laboratories for materials science and research

E-mail: arndt.remhof@empa.ch

http://www.empa.ch/h2e

Improvement of soft magnetic properties in $\text{Fe}_{84-x}\text{B}_{10}\text{C}_6\text{Cu}_x$ alloy system

1. Microstructure

The X-ray diffraction patterns for annealed $\text{Fe}_{84-x}\text{B}_{10}\text{C}_6\text{Cu}_x$ alloy ribbons are shown in figure 1. The alloys are almost at amorphous state after annealing when $x=0.5-0.7$. Crystallization phase α -Fe is seen to precipitate partially as Cu content increase. The average grain size D estimated from Sherrer's relation is 15 nm for $x=1.0$ and 20 nm for $x=1.15$, respectively. When $x=1.3$, the precipitation of crystallization phase α -Fe is obvious. The volume fraction of the crystalline phase is about 30% for $x=1.0$, 35% for $x=1.15$ and 45% for $x=1.3$, respectively. Hence, Cu addition has a vital impact on the precipitation of α -Fe.

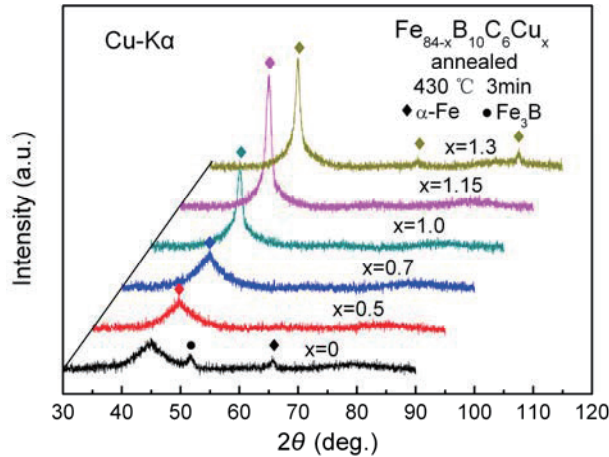


Fig. 1. X-ray diffraction patterns for annealed $\text{Fe}_{84-x}\text{B}_{10}\text{C}_6\text{Cu}_x$ alloy ribbons

2. Thermal properties

The DSC curves for $\text{Fe}_{84-x}\text{B}_{10}\text{C}_6\text{Cu}_x$ melt-spun ribbons are shown in figure 2. Here, T_{x1} and T_{x2} represent the crystallization temperature of α -Fe and the precipitation temperature of Fe-B compounds, respectively. According to the DSC data, T_{x1} decreases slightly with the increasing Cu content from $x=0$ to $x=1.15$. When $x=1.3$, T_{x1} decreases dramatically, the crystallization peak becomes broad and the crystalline behavior of bcc Fe occurs within a wide temperature range of about 100 °C, whereas T_{x2} shows little variation. Hence, the difference between T_{x1} and T_{x2} increases with the increasing x . Therefore, Cu addition takes important influence on the precipitation of the first phase and widens the crystallization temperature range.

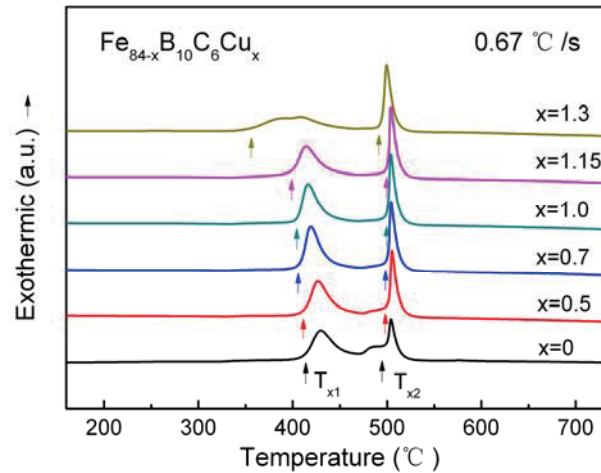


Fig.2. DSC curves for $\text{Fe}_{84-x}\text{B}_{10}\text{C}_6\text{Cu}_x$ melt-spun ribbons

3. Magnetic properties

Figure 3 shows Cu content x dependence of (a) coercivity H_c and (b) saturation magnetic flux density B_s of $\text{Fe}_{84-x}\text{B}_{10}\text{C}_6\text{Cu}_x$ alloys annealed at $430\text{ }^\circ\text{C}$ for 3 minutes. H_c decreases with the increasing x and exhibits a minimum at around $x=1.0$. Then H_c increases when $x=1.15-1.3$. This may be caused by the increasing grain size of the crystallization phase $\alpha\text{-Fe}$. While B_s shows an increasing tendency due to the precipitation of $\alpha\text{-Fe}$. So excellent soft magnetic properties got at $x=1.0$.

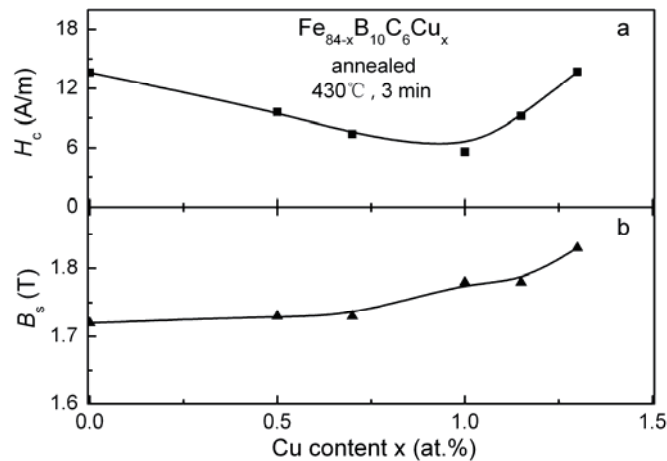


Fig.3. Cu content x dependence of (a) coercivity H_c and (b) saturation magnetic flux density B_s

In table 1, the B_s , H_c and core loss P of $\text{Fe}_{83}\text{B}_{10}\text{C}_6\text{Cu}_1$ nanocrystalline alloy under several conditions are compared with those of $\text{Fe}_{73.5}\text{Cu}_1\text{Nb}_3\text{Si}_{13.5}\text{B}_9$ and $\text{Fe}_{83.3}\text{Si}_4\text{B}_8\text{P}_4\text{Cu}_{0.7}$ nanocrystalline alloys and oriented Si-steel. The present alloy shows a lower H_c than $\text{Fe}_{83.3}\text{Si}_4\text{B}_8\text{P}_4\text{Cu}_{0.7}$ nanocrystalline alloy and oriented Si-steel. Although B_s shows a slightly decrease to these material, it is much higher than that of $\text{Fe}_{73.5}\text{Cu}_1\text{Nb}_3\text{Si}_{13.5}\text{B}_9$ nanocrystalline alloy. The high B_s is due to the high Fe content and not-containing any other metal elements such as Zr, Hf and Nb, which can lead to the

decreasing of B_s . Core loss of $P_{10/50}$ for $Fe_{83}B_{10}C_6Cu_1$ is 0.34 W/kg. That is about 80% of that of oriented Si-steel. What is more, the advantage of core losses at high frequencies such as $P_{10/400}$ and $P_{10/1k}$ compared to those of oriented Si-steel is obvious.

TABLE 1

The B_s , H_c and core losses of $Fe_{83}B_{10}C_6Cu_1$ nanocrystalline alloy under several conditions are compared with those of $Fe_{73.5}Cu_1Nb_3Si_{13.5}B_9$ and $Fe_{83.3}Si_4B_8P_4Cu_{0.7}$ nanocrystalline alloys and oriented Si-steel.

Material	B_s (T)	H_c (A/m)	$P_{10/50}$ (W/kg)	$P_{10/400}$ (W/kg)	$P_{10/1k}$ (W/kg)
$Fe_{83}B_{10}C_6Cu_1$	1.78	5.1	0.34	4.3	12.5
$Fe_{73.5}Cu_1Nb_3Si_{13.5}B_9$	1.24	0.53	$P_{2/20k}=2.1$		
$Fe_{83.3}Si_4B_8P_4Cu_{0.7}$	1.88	7	0.12		
Oriented-Si steel	2.03	8	0.41	7.8	27.1

Here, the symbols $P_{10/50}$, $P_{10/400}$ and $P_{10/1k}$ stand for core losses at 1.0T at 50 Hz, 400 Hz and 1k Hz, respectively.

Contact to

Baolong Shen (Ningbo Institute for Materials Technology & Engineering Chinese Academic of Science)

E-mail: blshen@nimte.ac.cn

<http://english.nimte.cas.cn/pe/fas/>

A feasibility study on HTS SMES applications for power quality enhancement through both software simulations and hardware-based experiments

Abstract

SMES system provides higher efficiency and faster response of charging and discharging energy. Thus it can be utilized as a power quality enhancement device especially in connection with renewable energy sources. In this report, a software simulation and an experiment result aiming at power quality enhancement are described. The study was performed using PSCAD/EMTDC and power-hardware-in-the-loop simulation scheme.

1. Power network configuration

The number of charging and discharging cycles of SMES is not limited [1–3]. Because of these advantages, various scales of HTS SMES projects have been carried out around the world [4, 5]. The model power network includes five generators as shown in Fig. 1. All generators were operated in governor free mode and the speed droop values were referred to IEEE Std. 1207TM-2004. The type of WPGS is a 600 kW squirrel cage induction generator (SCIG).

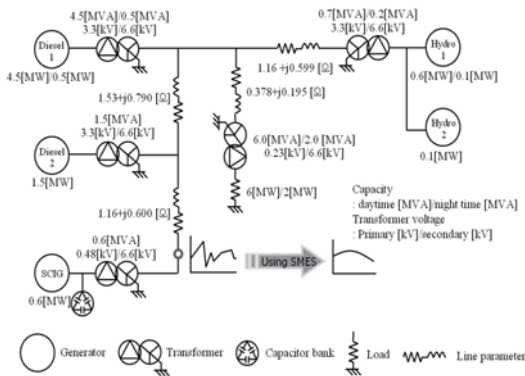


Fig. 1. Schematic diagram of the model power network including WPGS

2. PSCAD/EMTDC simulation

A software based simulation of the model power network including SMES was performed using PSCAD/EMTDC. Fig. 2 describes the control block diagram of the SMES system connected to the terminal of WPGS with DC/AC converter and DC/DC chopper. The SMES system is represented as an inductor in the simulation circuit.

At night, the capacity of the WPGS occupies about 21% of the total capacity of the generator and wind velocity varies between 7 m/s and 12 m/s on average. Consequently, the frequency fluctuation of the system violates its allowed limits, 60 ± 0.2 Hz. The energy capacity of the SMES was selected as 1 MJ and 2.5 MJ, and rated current was 450 A and 944 A, respectively. Fig. 3 represents the stabilization results for the utility frequency. It is clearly seen that the 2.5 MJ SMES can suppress the frequency fluctuations within the allowed limits.

3. Power-hardware-in-the-loop simulation

During the software simulation, the SMES is represented as only an inductor with operating current. To monitor not only the temperature variations but also

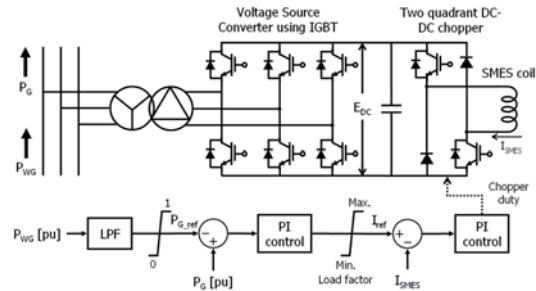


Fig. 2. Simulation circuit in PSCAD/EMTDC: Control diagram of DC/DC chopper for SMES system

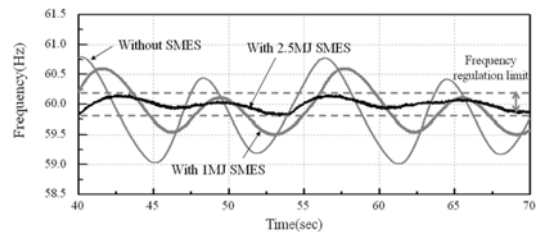


Fig. 3. Comparison of load side frequency stabilized by 1 MJ and 2.5 MJ SMES systems

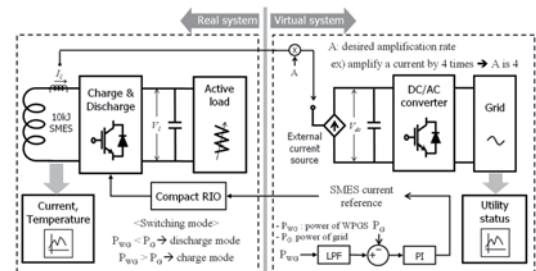


Fig. 4. Conceptual diagram of PHILS with RTDS and a real HTS SMES

operational characteristics of the SMES, PHILS was implemented. Fig. 4 shows a conceptual diagram of PHILS using RTDS and a real SMES [6].

The model power network was simulated using RTDS with the manufactured 10 kJ toroid-type HTS SMES and it was amplified as 2.5 MJ SMES in this simulation circuit. Fig. 5 depicts the hardware system which consists of a toroid-type HTS SMES, a DC/DC chopper. The toroid-type HTS SMES consists of a cryocooler for conduction cooling, metal current leads of brass between room temperature and cryogenic temperature condition, and HTS current leads made of coated conductor [6, 7].

Fig. 6 shows the utility frequency stabilized by the SMES system. The 10 kJ toroid-type HTS SMES was initially charged to 150 A, and consequently 2.5 MJ SMES in RTDS was initially charged to 600 A in RTDS. During the PHILS, the variations of the temperature of 10 kJ toroid-type HTS SMES were monitored in real time as shown in Fig. 7. The temperature varied according to the current charge and discharge, and the maximum temperature of one of the double pancake coils increased up to 9.2 K.

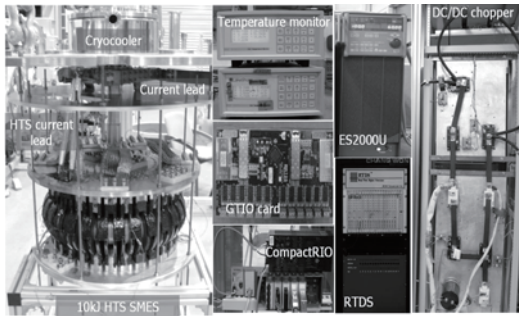


Fig. 5. 10kJ toroid-type HTS SMES and DC/DC chopper

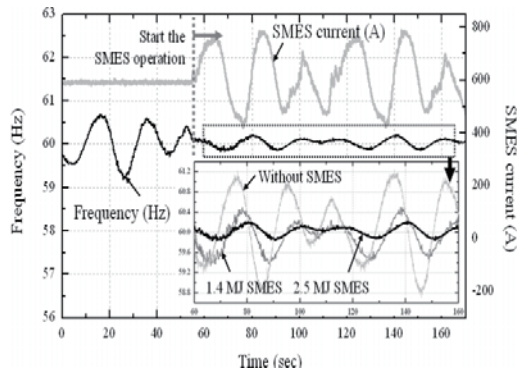


Fig. 6. Utility frequency stabilized by the SMES system and the variation in the current of the SMES using PHILS technology

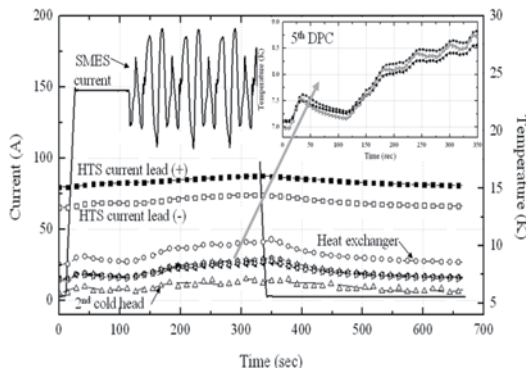


Fig. 7. Variations in the temperature of the SMES due to the operating current variations during compensating the fluctuation of utility frequency

4. Discussions

In this paper, software-based simulation and experiments aiming for power quality enhancement were performed to demonstrate the feasibility of the SMES system. According to the software-based simulation results, it is concluded that the 2.5 MJ SMES can be utilized to the model power network for frequency stabilization. Through the PHILS results, it is possible to monitor both power network status and operating conditions of the SMES system at the same time. Both results confirmed that a SMES system can possibly be utilized to enhance power quality in connection with renewable energy sources.

At present, a 2.5 MJ toroid-type HTS SMES is being manufactured in Korea. Using the current variation as shown in Fig.6, the losses such as eddy current loss and magnetization loss of the 2.5 MJ SMES can be calculated when it will be used for frequency stabilization. Furthermore, operational characteristics of not only 2.5 MJ toroid-type HTS SMES but also all types of SMES will be able to be predicted with higher reliable results through both software simulations and hardware-based experiments.

References

- [1] Cesar A. Luongo, IEEE Trans. 32 (1996) 2214.
- [2] Mohd. Hasan Ali, Bin Wu, Roger A. Dougal, IEEE Trans. 1 (2010) 38.
- [3] A.R. Kim, G.H. Kim, J.H. Kim, M. H. Ali, M. Park, I.K. Yu, H. J. Kim, S. Kim, K.C. Seong, IEEE Trans. 18 (2008) 705.
- [4] H. K. Yeom, S. J. Park, Y. J. Hong, D.Y. Kho, K. C. Seong, H. J. Kim, T.B.Seo, IEEE Trans. 18 (2008) 741.
- [5] P. Tixador, M. Deleglise, A. Badel, K. Berger, B. Bellin, J. C. Vallier, A. Allais, and C. E. Bruzek, IEEE Trans. 18 (2008) 1967.
- [6] A.R. Kim, G.H. Kim, K.M. Kim, J.G. Kim, M. Park, I. K. Yu, H.J. Kim, S.H. Kim, K. Sim, K.C. Seong, IEEE Trans. 20 (2010) 1339.
- [7] A.R. Kim, S.Y. Kim, K.M. Kim, J.G. Kim, M. Park, I.K. Yu, S. Lee, S. Kim, M. H. Sohn, H. J. Kim, J. H. Bae, K.C. Seong, Proceedings of the Applied Superconductivity Conference (ASC2010), August 1-6, 2010, Washington D.C.

Keywords

Power quality, Real time digital simulator, Superconducting magnetic energy storage

Contact to

In-Keun Yu
Changwon National University, Changwon , 641-773, Korea
E-mail: yui@changwon.ac.kr

Effects of deposition conditions on the structural features of CeO₂ films prepared by laser chemical vapor deposition

From January to March 2011, I visited IMR of Tohoku University to work on the laser chemical vapor deposition of CeO₂-based films in collaboration with Prof. T. Goto. We studied the influence of deposition conditions on microstructure, orientation and deposition rates of CeO₂-based films.

The most notable property of CeO₂ is its capacity to release and store considerable amounts of oxygen while preserving its fluorite structure, a property known as the oxygen storage capacity (OSC) [1]. CeO₂ is known to experience Ce⁴⁺ to Ce³⁺ reductive and Ce³⁺ to Ce⁴⁺ re-oxidizing behaviors via charge compensating oxygen vacancy mechanisms. This property makes CeO₂ a technologically useful oxide. The growth of CeO₂ films is one alternative for enhancing the OSC. Favorable oriented films are of significant importance not only in semiconductor industry [2-3] but also in catalysis [4-6]. As a buffer layer, (100)-oriented CeO₂ films are attractive to achieve the preferred (100) epitaxial growth of semiconducting films. (100)-oriented films are also catalytically desirable since the CeO₂ (100) plane is unstable compared with (111) and (110) planes and consequently more reactive. In addition, the formation of oxygen vacancies on CeO₂ (100) plane requires less energy than on (111) plane, which is directly related to the OSC [7]. A highly porous morphology and the natural defective film structure may further enhance the catalytic performance of CeO₂ by facilitating the oxygen mobility and increasing the accessible catalytic sites.

CeO₂-based films were prepared on silica glass substrates (10 mm × 15 mm × 1 mm) in a hemispherical cold-wall type LCVD apparatus. A semiconductor InGaAlAs (808 nm in wavelength) laser beam was defocused to about 20 mm in diameter to irradiate the whole substrate. Ce-dipivaloylmethanate [Ce(dpm)₄] was employed as precursor. It was evaporated at 493 - 533 K and their vapors were carried by argon gas (flow rate: 50 - 200 cm³/min) through a vertical nozzle separated 25 mm from the substrate. Oxygen gas was added (flow rate: 50-200 cm³/min) through a concentric-vertical nozzle and mixed with the precursor vapors just above the surface substrate. Before deposition, the substrates were pre-heated (T_{pre}) from 473 to

873 K. While the laser power (P_L) was controlled from 0 to 200 W, the total pressure (P_{tot}) was varied from 0.4 to 0.8 kPa. Depositions were performed for 600 s. Deposition rates were estimated from cross-sectional film images. The crystal structure of the films was analyzed by typical θ -2 θ X-ray diffraction measurements (XRD; Rigaku RAD-2C). The surface morphology and cross-sectional microstructures were investigated by field emission scanning electron microscopy (FESEM; JEOL JSM-7500F) and transmission electron microscopy (TEM; JEOL 2000 EXII, 200 kV).

Figure 1 summarizes the effects of T_{pre} and P_L on the structural features of CeO₂ films over the entire ranges investigated. P_{tot} was kept at 0.8 kPa. Without the influence of laser irradiation, i.e. $P_L = 0$, non-oriented films were obtained above $T_{pre} = 573$ K. In contrast, (100)-oriented films were often produced under the influence of laser irradiation even without the need of pre-heating (R.T.), when $P_L = 150 - 200$ W. Feather-like columnar grains were typically observed at oriented films, while those prepared at $P_L = 200$ W and especially at $T_{pre} = 873$ K exhibited dense and wider columns.

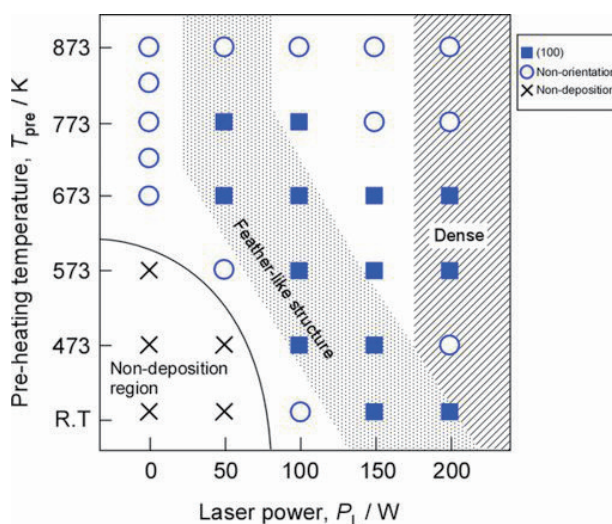


Figure 1. Effects of T_{pre} and P_L on the structural features of CeO₂ films.

Figure 2 presents the FESEM images of the cross-sectional structure and surface morphology of CeO₂ films prepared at $T_{pre} = 673$ K, $P_L = 50 - 150$ W and $P_{tot} = 0.8$ kPa. A clear columnar structure was developed under laser irradiation, where the columns exhibited either pyramidal or flat top-endings mainly depending on P_L

conditions. Pyramidal ending columns were predominantly exposed. At $P_L = 0$, grains with no specific orientation and rather granular surface morphology were typically observed. Since the precursor vapors and the surface mobility of chemical species could be highly activated by laser irradiation, enhanced selective adsorption of oxygen on more reactive (100) surface may be accounted for a faster growth along [100] direction from initially randomly oriented grains.

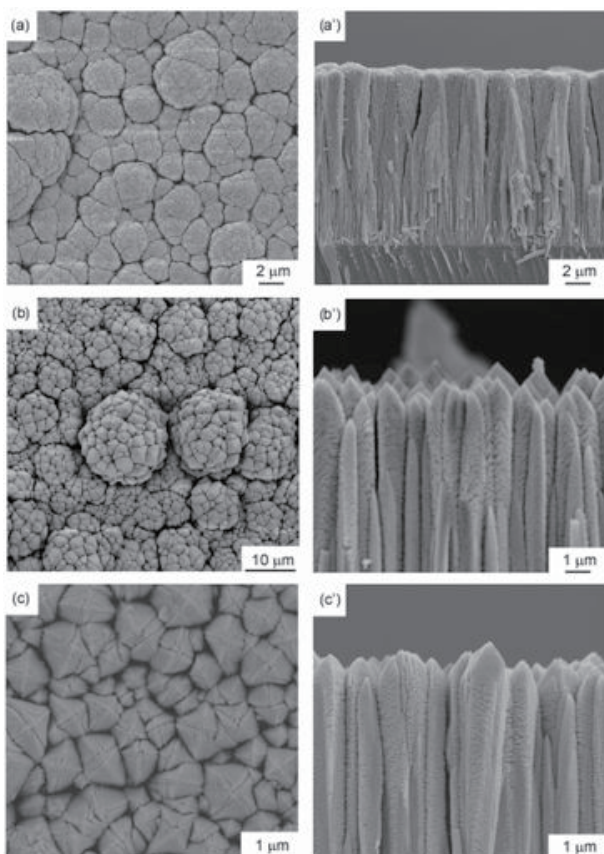


Figure 2. FESEM images of the cross-sectional structure and surface morphology of CeO_2 films prepared at $T_{\text{pre}} = 673\text{K}$, (a) $P_L = 150$, (b) $P_L = 100$ and (c) $P_L = 50$ W.

Figure 3 shows the change of Lotgering factor (100) for CeO_2 films as a function of P_L and T_{pre} . Lotgering factor achieved values above 0.8 for most conditions producing oriented films. This implies a high degree of (100) orientation and the ability of LCVD to growth desirable oriented CeO_2 films. At $P_{\text{tot}} = 0.4 - 0.6$ kPa, however, films showed not only (100) but also (110) and (311) orientations. In summary, (100) preferred orientation was obtained at high total pressure ($P_{\text{tot}} = 0.8$ kPa) over the entire range of temperature ($T_{\text{pre}} = 473 - 873$ K), while (110) and (311) orientations were produced at low total pressure ($P_{\text{tot}} = 0.4 - 0.6$ kPa).

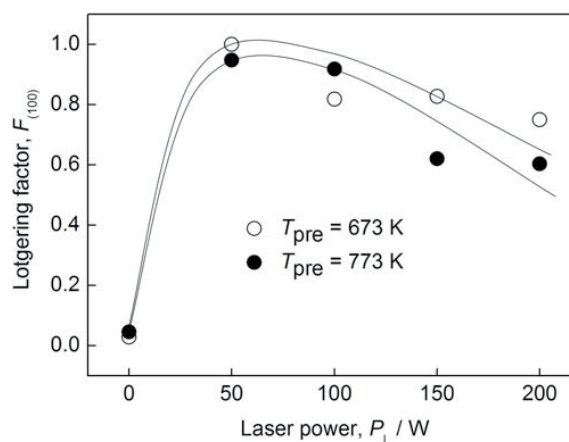


Figure 3. Change of Lotgering factor (100) for CeO_2 films as a function of P_L and T_{pre} .

References

- [1] A. Trovarelli, Catal. Rev. Sci. Eng. 38 (1996) 439.
- [2] P. Zhao, A. Ito, R. Tu, T. Goto, Appl. Surf. Sci. 256 (2010) 6395.
- [3] S. Liang, C.S. Chern, Z.Q. Shi, P. Lu, Y. Lu, B.H. Kear, J. Cryst. Growth 151 (1995) 359.
- [4] X. Wang, J.A. Rodriguez, J.C. Hanson, D. Gamarra, A. Martinez-Arias, M. Fernandez- Garcia, J. Phys. Chem. B 109 (2005) 19595.
- [5] Q. Liang, X. Wu, D. Weng, H. Xu, Catal. Today 139 (2008) 113.
- [6] J.A. Rodriguez, J.C. Hanson, J.-Y. Kim, G. Liu, A. Iglesias-Juez, M. Fernandez-Garcia, J. Phys. Chem. B 107 (2003) 3535.
- [7] J.C. Conesa, Surf. Sci. 339 (1995) 337.

Acknowledgements

I wish to express my gratitude to Prof. A. Inoue and Prof. T. Goto for the invitation to IMR of Tohoku University and for all the facilities and support. I also extend my thanks to Prof. T. Rong for his immense help in every step of this research.

Key Words

Laser chemical vapor deposition, CeO_2 films, Oriented films

Contact to

Jorge Roberto Vargas Garcia (Metallurgy and Materials Eng. Department, National Polytechnic Institute, Mexico)

E-mail: rvargasga@ipn.mx

Activity Report

Workshops



FY 2010 Workshops

No.	Chairperson	Title of Workshop	Place	Date
10WS1	T. Goto	The 5th International Workshop on Bio and Amorphous Materials,	Zao, Miyagi	2010.8.9-8.10
10WS2	M. Fujita	•Recent Progress on Spectroscopies and High-Tc Superconductors	IMR Lecture Hall	2010.8.9-8.11
10WS3	Y. Kawazoe	The 5th General Meeting of ACCMS-VO	IMR Lecture Hall	2010.12.10.12.12

Recent Progress on Spectroscopies and High- T_c Superconductors

In this workshop, we discuss the prospect of future development in the quantum beam spectroscopy with selecting the cuprate and iron-based high- T_c superconductors as main target systems. Various views among experimental and theoretical studies have been exchanged. We confirmed the importance of complementary use of quantum beam spectroscopy to clarify the peculiar charge and spin dynamics.

The international workshop “Recent Progress on Spectroscopies and High- T_c Superconductors” was held on August 9th-11th, 2010 in Lecture Hall of Institute for Materials Research (IMR), Tohoku University. This workshop aimed to discuss the recent progress on condensed matter physics brought by quantum beam spectroscopy measurements. Main topic was superconductivity in the iron-based superconductors and high- T_c cuprates, for which various challenging experimental and theoretical techniques are adapted to clarify exotic electronic states in these materials. Especially, the mechanism of superconductivity in Fe-based compounds, which was discovered by Hosono group in Japan [1], has been attracted much attention due to the possible novel physics and possibility of higher- T_c in related materials. In addition to the discovery of new compounds, the world top-class experimental facilities such as synchrotron radiation facility (SPring-8) and high intensity proton accelerator facility (J-PARC) provide a great opportunity to elucidate the overall picture of electronic states in intriguing materials. Therefore, the broad discussion on recent progress of quantum beam spectroscopy is very important for the new era of condensed matter physics.

There were 35 oral presentations (28 experimental and 7 theoretical works) and 90 researchers participated in the work-



Fig. 1. A picture of workshop. 90 researchers including many young scientists participated in the workshop and exchanged the information.

shop. We invited 11 outstanding speakers from abroad, who introduced many new results and overviews on superconductors. The research results in the exciting field of iron related materials were discussed to share what are important issues to reveal the high- T_c mechanism in this system. The complementary use of quantum beam spectroscopy, e.g. neutron, X-ray, Raman, photoemission, STM/STS, NMR, and mu-SR, was also discussed, since it is necessary to study the multi-structure of the electronic states in the real, momentum and energy spaces. The participants actively discussed and exchanged the information during the workshop. We summarized huge amount of information on transition metal based superconductors and contributed to extract essential points among them. A booklet collecting slides presented in this workshop was distributed to the participants and the information benefits researchers on above subjects. This workshop received favorable impressions and opinions from the participants.

The workshop was supported by,

- 1) International Collaboration Center (ICC-IMR), IMR, Tohoku University,
- 2) Collaborative Research Project, IMR, Tohoku University,
- 3) Grant-in-Aid for Specially Promoted Research in MEXT, Japan
“Development of the 4 Space Access Neutron Spectrometer (4 SEASONS)
and Elucidation of the Mechanism of High- T_c superconductivity (17001001)”
- 4) Advanced Science Research Center, Japan Atomic Energy Agency.

We would like to thank all participants for their active contributions in the workshop.

References

- [1] Y. Kamihara et al., J. Am. Chem. Soc. 130, 3296 (2008).

Key Words

Quantum Beam spectroscopy, neutron-scattering, J-PARC, SPring-8, High- T_c superconductor, Iron Pnictide superconductor

Contact to

Masaki Fujita (Materials Processing and Characterization Division)

E-mail: fujita@imr.tohoku.ac.jp

<http://www.yamada-lab.imr.tohoku.ac.jp/jp/index.html>

Highlight of ICC-IMR International Workshop The 5th General Meeting of Asian Consortium on Computational Materials Science – Virtual Organization (ACCMS-VO) Dec. 10-13, 2010, Chairperson Y. KAWAZOE (IMR)

This is the 5th annual meeting of “off the net” of the virtual organization for computational materials scientists mainly in the Asian region, who are working collaboratively daily via international computer network using our supercomputer at the Center for Computational Material Science, Institute for Materials Research, Tohoku University (CCMS, IMR, TU). The audiences celebrate the 10th anniversary of the ACCMS, which started in Sendai with only 16 researchers from Japan, China, India, Russia, Thai, Iran, US, and Canada. In these 10 years 5 main meetings in India, Russia, China, Korea, and Vietnam, 5 VO meetings, and 3 WG meetings in Singapore, Korea, and Sendai, were held. Especially VO meetings have been held in Sendai continuously every year. We have published the Proceedings for all the main meeting including invited talks and some of the oral talks from international journal publishers. The present meeting focuses on designing efficient hydrogen storage materials and new methodologies in computational materials science, using the supercomputer at IMR and other member institutions aiming to use the Computer K in Kobe. About 120 researchers from 13 countries gathered supported by ICC-IMR and other organizations, and not only present their recent research results and exchange ideas but also mixed up to start new collaborations among them. This meeting is really international. Although many so-called international conferences in Japan accommodate only several foreign speakers, our meetings always have a number of foreigners and enjoy mixing different cultures here in Sendai to establish good and deep understanding with each other. These new international collaborations will be continued on the computer network to establish ACCMS-VO as a research basis of the members. The details of the meeting and activities are open through our ACCMS webpage; please check <http://www-lab.imr.edu/~accmsvo5/index.html>.

The list of invited talks are shown below, which covers the recent important area in computational materials science and technology, and some of them will be published as a book form from Springer-Verlag to celebrate the 10th anniversary of the ACCMS society.

- 1: Marcel H.F. Sluiter (Delft University of Technology), “*Ab initio* Predictions of the Various Roles of Substitutional Alloying Elements in Low-alloyed Ferritic Steel”
- 2: Keivan Esfarjani (Massachusetts Institute of Technology), “Thermal Conductivity of Bulk Crystals from First-principles”
- 3: Jian-Tao Wang (Chinese Academy of Sciences), “Magic Monatomic Linear Chains for Mn Nanowire Self-Assembly on Si(001)”
- 4: Sang Uck Lee (LG Chem, Ltd / Research Park), “The Origin of the Strain Energy Minimum in Imogolite Nanotubes”
- 5: S. Vannarat (National Electronics and Computer Technology Center), “Storm Surge Simulation in the Gulf of Thailand with Finite Volume Coastal Ocean Model”
- 6: Jer-Lai Kuo (Academia Sinica), “On the Development of A First-Principle Based Multi-model Method to Study Aqueous Systems: from Clusters, Interfaces to Condensed Phases”
- 7: Bing-Joe Hwang (National Taiwan University of Science and Technology), “Combined Experimental and Theoretical Investigation of Nanosized Effects of Pt Catalyst on Methanol Electro-Oxidation Activity and Pt-O and Pt-OH Stability in Oxygen Reduction Reaction”
- 8: H. M. Weng (Chinese Academy of Sciences), “Pressure Induced Superconductivity in Topological Compound Bi₂Te₃”
- 9: John Maguire (The U.S. Air Force Research Laboratory), “Computer Methods in Nanomanufacturing”

- 10: Vu Ngoc Tuoc (Hanoi University of Science and Technology), "Molecular Dynamics Study on Strain Distribution and Mechanical Properties of Si/Ge Heterostructure Nanowire along the [111] Direction"
- 11: Kwang-Ryeol Lee (Korea Institute of Science and Technology), "Molecular Dynamics Simulations of Amorphous Carbon Film Growth"
- 12: Gang Chen (University of Jinan), "Structural and Electronic Properties of Neutral and Charged Ca₈C₁₂ Metal Carbides"
- 13: Abhishek K. Singh (Indian Institute of Science), "Digging Wells in Graphane to Mine Graphene Roads and Quantum Dots"
- 14: Umesh V. Waghmare (Jawaharlal Nehru Centre for Advanced Scientific Research), "Soft Modes, Hyperelasticity, and Crack Instability: Elastodynamic Analysis from First-principles"
- 15: G. P. Das (Indian Association for the Cultivation of Science), "How do 3d Transition Metal Clusters Behave When Encapsulated Inside BN Cages and Nanotubes?"
- 16: H. Chen (Fudan University), "Edge States and Electronic Devices in Graphene Nanoribbons"
- 17: Michael R. Philpott (University of California Berkeley), "Multi-radical Ground State and Magnetism of Neutral, Charged and Chemically Modified Zigzag Edged Graphene Nanopatches"
- 18: K. Iyakutti (Madurai Kamaraj University), "Investigation of Wigner Crystallization in Graphene"
- 19: Vijay Kumar (Dr. Vijay Kumar Foundation), "Band-gap Engineering of Graphene by BN Doping and Effects of Metal Contacts: *Ab-initio* Calculations"
- 20: Masanori Tachikawa (Yokohama City University), "Path Integral Simulation for Hydrogen Bonded Systems: Protonic Quantum Nature and H/D Isotope Effect"
- 21: Shin-ichi Orimo (Tohoku University), "Hydrogen Storage and Ionics in Complex Hydrides"
- 22: Yuan Ping Feng (National University of Singapore), "Stabilizing Metal Atoms and Clusters on Graphene for Catalytic and Hydrogen Storage Applications"
- 23: V. R. Belosludov (Tohoku University), "Prediction of Structure, Composition and Phase Behavior of Helium Clathrate Hydrates"
- 24: Qiang Sun (Peking University), "Enhancing Hydrogen Storage with an Applied Electric Field"





Activity Report

KINKEN WAKATE



FY 2010 KINKEN WAKATE

No.	Chairperson	Title of Workshop	Place	Date
10Wakate	K. Fujiwara	10th Materials Science School for Young Scientists (KINKEN-WAKATE 2013)	TRUST CITY CONFERENCE	2013.11.21-22

KINKEN-WAKATE 2010

Abstract: 7th Materials Science School for Young Scientists (KINKEN-WAKATE 2010) was held on December 2-3, 2010 in Sendai. Totally 91 people, including 83 graduate students and postdoctoral fellows were attended and enjoyed enthusiastic discussions on materials sciences.

The 7th Materials Science School for Young Scientists (KINKEN-WAKATE 2010) was subtitled as "Challenge of radiation for advanced materials science". This is a message for attendees so that energetic radiations induce quite interesting phenomena which result in degradation of materials' properties as well as in introduction of non-equilibrium phase. Both are indispensable for evaluations of materials lifetime and for development of new materials, respectively.

Based on the idea, the organizers invited the following lectures from Japan, US and France:

- Dr. Pascal Garin (IFMIF/EVEDA Project Leader, International Fusion Energy Research Centre),
- Dr. Roger E. Stoller (Oak Ridge National Laboratory),
- Prof H. Yamana (Kyoto University), and
- Prof H. Yasuda (Osaka University).

Applications from graduate students and postdoctoral fellows were finally 83. The contents were 12 from IMR, 6 from Graduate School of Science, 63 from Graduate School of Engineering, and 2 from Graduate School of Environmental Studies. 52 foreign students and postdocs were from 13 countries.

The program is as follows:

December 2nd (Thu)

13:00-13:15 Opening Remark: T. Goto (Chair of KINKEN-WAKATE, IMR)

13:15-14:15 Lecture 1: Dr. R.E. Stoller "Modeling radiation-induced microstructural evolution: different phenomena at different length and time scales"

14:15-15:15 Lecture 2: Prof. H. Yamana "Importance of advanced material research and heavy element chemistry for the successful use of nuclear energy in the future"

15:30-17:00 Poster Preview of Session A (2 min × 42)

17:00-18:30 Poster Session A

21:00-22:00 Free Discussion

December 3rd (Fri)

9:00-10:30 Poster Preview of Session B (2 min × 42)

10:30-12:00 Poster Session B

13:30-14:30 Lecture 3: Dr. Pascal Garin "Nuclear Fusion Energy and its Developments (ITER, IFMIF, DEMO)"

14:30-15:30 Lecture 4: Prof. H. Yasuda "Electron-irradiation-

induced phase transformations by TEM"

15:45-16:15 Closing & Poster Award

The lectures nicely summarized science of radiation effects in computer sciences, chemistry and electron microscopy, as well as engineering issues in nuclear energy and fusion energy. Quite a many of questions and discussions were raised to the lectures.

This time of KINKEN-WAKATE, poster preview sessions were arranged. They are 2-minute short presentations prior to the poster sessions. Poster sessions and the preview sessions were evaluated by 8 professors and nominated the following 8 young scientist for the best poster award:

Mr. M. Miyake "Development of Co-based alloy tools for friction stir welding of steels and Ti alloys",

Dr. S. Bosu "Observation of spin Seebeck effect in half-metallic full-Heusler alloy Co_2MnSi thin film",

Dr. L.H. Bai "Control of spin waves coupling through a DC current",

Mr. J.H. Choi "Comparisons of optical properties between polar and non-polar $InGaN/GaN$ multiple-quantum-well light-emitting-diodes",

Mr. H. Kurita "Observation of CNT-AI interface in CNT/AI composite fabricated by spark plasma sintering/hot extrusion hybrid process",

Ms. L. Zhang "Wrinkled nanoporous gold films with ultrahigh SERS enhancement",

Mr. T. Kawamata "Structural study of the $Zr_{70}X_{30}$ ($X=Cu, Ni, Pd$) amorphous alloys by the AXS-RMC analysis", and

Ms. S. Komiyama "Effect of Heat Treatment on the Microstructure and Wear Properties of Ti-Mo-N films with Low Nitrogen Content".

We appreciate all participants for their contributions leading great success of this school.



Figure 1. KINKEN-WAKATE 2010 group photo

Contact to

Hiroaki ABE and Yasuyoshi NAGAI (IMR)

E-mail: abe.hiroaki@imr.tohoku.ac.jp

E-mail: nagai@imr.tohoku.ac.jp

<http://www-lab.imr.tohoku.ac.jp/~wakate2010/index.html>

Activity Report

Short-term Visiting Researchers



FY 2010 Short-term Visiting Researchers

Application No.	Name	Host	Proposed Research	Title	Affiliation	Term
10SV1	Kwang-Yong Choi, Korea	H. Nojiri	Pulsed Field Magnetization of [Cu3] in Si Nanoporous	Assistant Professor	Chung-Ang University, Korea	2010.5.28-5.31
10SV2	Hyun-Seop Shin	S. Awaji	Electro-Mechanical Property Evaluation in HTS CC Tapes	Professor	Andong National University, Korea	2010.6.28-7.2
10SV3	Atsufumi Hirohata	K. Takanashi	Experimental Demonstration of a Persistent Current	Lecturer	University of York, UK	2010.7.28-8.8
10SV4	Jacob Ruff Zahirul Islam	H. Nojiri	Advanced High Field X-Ray Scattering Studies for Functional Magnetic Materials	Director's Postdoctoral Fellow Physicist	Argonne National Laboratory, USA	2010. 9.7-9.15
10SV5	Alexander Vasilev Olga Volkova	H. Nojiri	The Study of Magnetic Phase Diagram of New Triangular Lattice Compound CsFe3	Professor Senior researcher	Moscow State University, Russia	2010.10.19-10.30
10SV6	Kwang-Yong Choi	H. Nojiri	High-Frequency ESR Study of the Two-Leg Spin Ladder BiCu2PO6	Assistant Professor	Chung-Ang University, Korea	2010.12.16-12.23
10SV7	Christian Schroeder	H. Nojiri	Solving Large-Scale Scientific Problems Using Public Resource Computing	Professor	Univ of Applied Sciences Bielefeld, Germany	2010.11.20-11.25
10SV8	Ouyang Zhongwen	H. Nojiri	High-Magnetic-Field Measurements and Single Crystal Growth	Assistant Professor	Wuhan National Magnetic Field Center, Huazhong Univ. of Science and Technology, China	2011.1.15-1.20
10SV9	Umesh V. Waghmare	T. Nishimatsu	First-Principles and Molecular-Dynamics Simulations of Ferroelectrics	Professor	Jawaharlal Nehru Centre for Advanced Scientific Research, India	2011.1.4-1.10
10SV10	Masaaki Matsuda	K. Ohoyama	Study of Spin Correlations in Geometrically Frustrated Systems Using Polarized Neutron and Pulsed Magnetic Fields	Lead Instrument Scientist	Oak Ridge National Laboratory, USA	2011.1.2-1.9
10SV11	Urs Staub	Y. Narumi	Resonant Soft X-Ray Scattering Under Pulsed High Magnetic Fields	senior scientist	Paul Scherrer Institute, Switzerland	2011.2.20-2.23
10SV12	Gerrit E.W. Bauer	E. Saitoh	Theory of spin Seebeck effect	Professor	Delft University of Technology, The Netherlands	2011.2.2-2.9

Pulsed Field Magnetization of {Cu₃} in Si Nanoporous

Magnetization measurement was made on the {Cu₃} cluster in Si nanoporous, which is the candidate of the quantum qubit unit. We found the step like magnetization with hysteresis loop, which is similar to the bulk magnetization. The present result shows that the magnetic property of the cluster is unchanged by the absorption into the nanoporous and that such system can be used for the study of magnetic properties of independent clusters in solid shape.

Molecular nanomagnets provide attractive targets for the realization of quantum bits. Recently, the quantum oscillations between the ground and excited collective spin states (so-called Rabi oscillation) were observed in the {V₁₅} molecular clusters. The spin decoherence time amounts to an order of 100 μs at liquid helium temperature. However, the most of works have been done in a solution. This puts constraint on the scalability as a spin-based quantum memory.

To realize a molecular magnet qubit all decoherence sources should be identified and suppressed. Besides, for an ultimate application, molecular magnets should be incorporated into a modern semiconductor technology. We will consider triangle molecular nanomagnets {Cu₃} deposited in silicon nanoporous as a promising candidate.

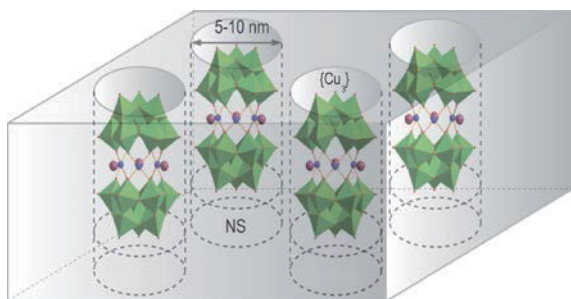


Fig. 1 Schematic view of Si-nanoporous with {Cu₃} .

Figure 1 shows the schematic view of Si-nanoporous compound. The size of the pore is adjusted to match the diameter of the {Cu₃} cluster. Thus, only single cluster can go into each pore. The average number of the cluster absorbed into nanoporous was estimated by measuring the change of weight. The standard measurement of magnetic susceptibility shows the drop of the effective Curie constant at low temperature. It suggests that the ground state of the cluster is $S=1/2$ as that of the bulk system. However, a magnetic property of the absorbed cluster is still unclear. Hence we have performed the magnetization measurement in high magnetic

field to examine the magnetic state of the {Cu₃} cluster. The experiment was done with a pulsed magnetic field and the lowest temperature was 0.5 K by using the ³He cooling system.

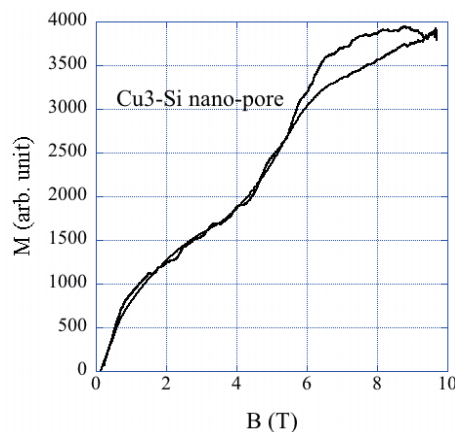


Fig. 2 Magnetization curve of {Cu₃} in Si-nanoporous at 0.5 K.

Figure 2 shows the magnetization curve of Si-nanoporous. We found a step like increase at 5 T, which is caused by the level crossing between the lowest doublets and the higher quartet. A clear hysteresis is also found above the level crossing. Those properties called "half-step" show the similarity with the bulk cluster. The half-step magnetization observed in the bulk {Cu₃} can be served as an indicator of a quenching of thermal relaxations. It means that the magnetic property of the absorbed cluster is unchanged in the process and the relaxation time is long.

This result together with ESR spectra enabled us to determine the spin Hamiltonian and energy levels in details. The obtained exchange coupling of Si:{Cu₃} shows the slight increase as indicated by the change of the crossing field. It may be caused by the stress given to the {Cu₃} from the Si environments.

In summary, we have examined the magnetization process of and {Cu₃} in Si-nanoporous and found that the major magnetic properties remain unchanged. It would contribute to examine the property of independent clusters in nanopores and to develop the candidates of qubit operation unit.

Key Words

High Magnetic field, molecular magnet, nano-material

Contact to Kwang-Yong Choi (Department of Physics, Chung-Ang University)

E-mail: kchoi@cau.ac.kr

Evaluation of Strain Effect on Critical Current under Magnetic field in REBCO Coated Conductor Tapes

The strain effect on the critical current, I_c under magnetic field in REBCO coated conductors has been evaluated. Differently processed CC tapes namely MOCVD-YBCO, RCE-SmBCO and EDDC-SmBCO showed good magnetic tolerance of I_c with different degradation behavior under magnetic field.

A commercially available MOCVD-YBCO CC tape from Superpower and two kinds of SmBCO CC tapes fabricated by the batch type EDDC process (evaporation on dual drum chamber) and the reel to reel RCE-DR process (reactive co-evaporation by deposition and reaction), respectively [1] were supplied for the test. All samples have Hastelloy substrate, and adopted IBAD process for grain alignment of the buffer layer and were Cu surround stabilized.

For the evaluation of the electromechanical property under magnetic field, a Katagiri type loading fixture was used [2]. Strain was measured using strain gauge and Nyilas-type extensometer simultaneously. These two strain sensing devices were adopted for comparison and to ease the burden in case one will not function properly under magnet field. In this test, strain gauges used have 0.2 mm gauge length and gauge factors of $1.88 \pm 1.5\%$ and $2.02 \pm 1.5\%$. Twin extensometers have gauge lengths of 12.5 and 14.5 mm, respectively. Strain gauges were attached axially along the load direction at both HTS and substrate surfaces. On the other hand, twin extensometer was clipped to the sample. Measurement of the strain effect on I_c under magnetic field in coated conductors was carried out at 77 K by using 15 T cryo-cooled superconducting magnet of HFSLM, IMR at Tohoku University. Critical current was measured using $1 \mu\text{V cm}^{-1}$ criterion. Sample length, gauge length and voltage tap separation were 40, 20 and 10 mm, respectively. Reversibility test was done by loading and unloading scheme. Magnetic field was applied to the sample parallel to the c-axis/perpendicular to the tape surface. Stress-free cooling was considered to prevent the contraction effect of different materials of the rig during cool-down from RT to 77K.

Fig. 1 shows the magnetic field dependence of normalized critical current, I_c/I_{c0} and it depicts that all CC tapes showed a significant I_c/I_{c0} degradation up to 3 T in which EDDC-SmBCO exhibits a much better magnetic field tolerance of I_c . Magnitude of I_c degradation at specific magnetic field value varies from each tape and this shows that the response of I_c to magnetic field depends not only on the kind of the superconducting layer but also on the fabrication process adopted. The difference may be attributed to the pinning mechanisms in each CC tapes.

Fig. 2-4 shows the I_c/I_{c0} -strain relation under magnetic field in MOCVD-YBCO, RCE-SmBCO and EDDC-SmBCO CC tapes, respectively. In the case of YBCO CC tape in Fig. 2, an interesting behavior can be observed showing shifting of the I_c peak location with magnetic fields as has been described in [3,4].

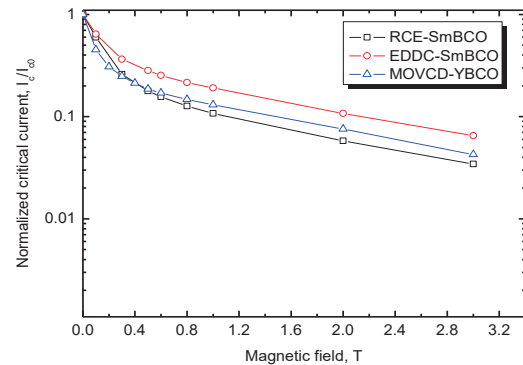


Fig. 1. Magnetic field dependence of I_c/I_{c0} in REBCO coated conductor tapes.

The I_c peak shifted from 0.1% to around 0.3% from 0 T to 0.5 T, respectively which means that the location of these I_c peaks are not solely determined by the residual strain at the HTS film. The I_c/I_{c0} -strain curves deviate from the 0 T curve in two ways. The curve moves upward up to about 0.5 T and then moves downward as the magnetic field increases. The magnetic field boundary of these two behaviors can be found between 0.3 and 0.5 T. Degradation of I_c/I_{c0} at 0 T and 3 T showed almost the same behavior.

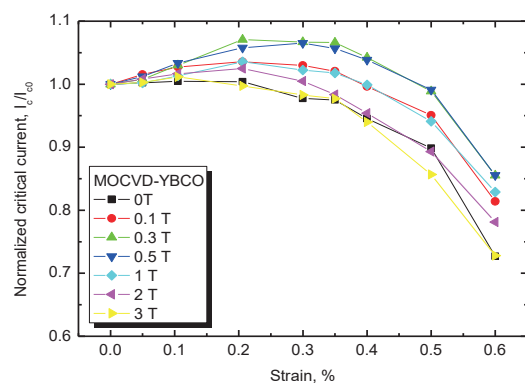


Fig. 2. Normalized critical current, I_c/I_{c0} as a function of uniaxial strain under different magnetic field in MOCVD-YBCO CC tape

On the other hand, in the cases of SmBCO CC tapes specifically in RCE-SmBCO, the I_c/I_{c0} showed different behavior.

In both SmBCO CC tapes, no I_c peak was observed during

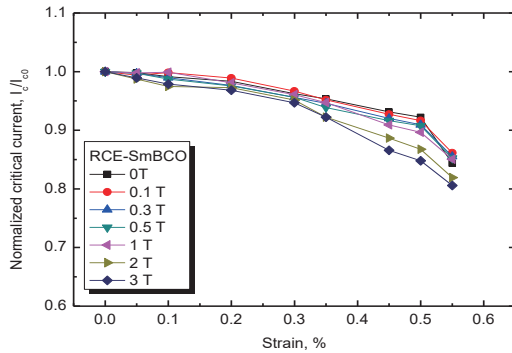


Fig. 3. Normalized critical current, I_c/I_{c0} as a function of uniaxial strain under different magnetic field in RCE-SmBCO CC tape.

tension showing a monotonic decrease of I_c/I_{c0} with strain in contrast to the case of YBCO CC tape. As can be seen in Fig. 3, I_c/I_{c0} decreased gradually with magnetic field. Degradation of I_c/I_{c0} became a little significant at higher magnetic field over 2 T. Fig. 4 shows the result for EDDC-SmBCO CC tapes. At 0.35% strain using strain gauge, I_c decreased abruptly. At this point, strain gauge did not function well and when the extensometer strain values were checked it showed that the abrupt I_c decrease was because the CC tape exceeded its yield strain. During the test, continuous increase in strain at high magnetic field was observed thus entering the plastic deformation region. Therefore, in the case of EDDC-SmBCO CC tapes, further test is necessary to check the influence of the substrate material and to obtain a more reliable result as some scattering of data is observed.

For the reversibility test under magnetic field, all of the samples

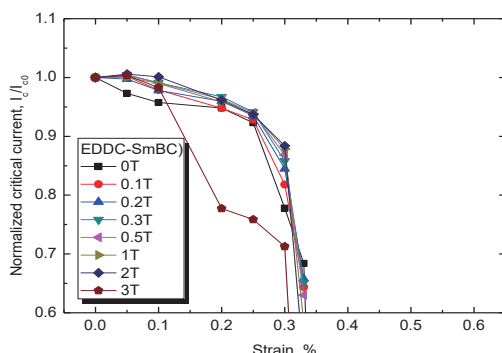


Fig. 4. Normalized critical current, I_c/I_{c0} as a function of uniaxial strain under different magnetic field in EDDC-SmBCO CC tape.

showed a reversible behavior up to some strain values around 0.5% which is comparable to the cases under self-field. We can infer that the reversibility strain tolerance of CC tapes here

tested is independent on the magnetic field up to certain values considered in this test.

The magnitude of the strain effect on I_c depends on magnetic field. Results showed that the I_c/I_{c0} -strain behavior was different in YBCO and SmBCO CC tapes. The difference is mainly due to the intrinsic properties of each superconducting film layer namely YBCO and SmBCO although similar substrate material may also show a different degree of magnetic tolerance behavior as have been presented here.

References

- [1] H. S. Ha, H. S. Kim, J. S. Yang, Y. H. Jung, R. K. Ko, K. J. Song, D. W. Ha, S. S. Oh, H. K. Kim, K. K. Yoo, C. Park, D. J. Youm, S. H. Moon, and J. H. Joo, *Physica C*, 463-465 (2007) 493-496.
- [2] G. Nishigima, K. Minegishi, K. Watanabe, K. Ohata, K. Nagawa, G. Iwaki, *IEEE Trans. Appl. Supercond.* 20 (2010) 1391-1394.
- [3] M. Sugano, T. Nakamura, T. Manabe, K. Shikimachi, N. Hirano, S. Nagaya, *Supercond. Sci. Tech.*, 21, (2008).
- [4] D. C van der Laan, J. W. Ekin, J. F. Douglas, C. C. Clickner, T. C. Stauffer, L. F. Goodrich, *Supercond. Sci. Technol.* 23 (2010).

Key Words

Strain effect, critical current, YBCO, SmBCO, magnetic field dependence

Contact to

Hyung-Seop Shin (Professor of Department of Mechanical Design Engineering, Andong National University)

E-mail: hsshin@andong.ac.kr

<http://home.andong.ac.kr/mdesign/index.htm>

Experimental demonstration of a persistent current

We report our experimental evidence of the spin-polarised persistent current in a Au nanoring under a non-uniform field generated by an FePt nanopillar under its remanent state. This is the first experimental demonstration of such a current theoretically predicted by Loss and Goldbart [1].

Spintronic nanostructures have a great potential to reveal additional quantum phenomena and hence have been intensively investigated to realise such quantum spintronic devices at room temperature. As a first step towards such devices, detailed characterisation on nanodevices need to be carried out at very low temperature, where quantum phenomena are expected to appear. For example, a persistent current has been theoretically predicted to flow in a non-magnetic nanoring under an asymmetric perpendicular magnetic field [1].

In this study, a new method to fabricate a quantum device, consisting of an FePt nanopillar and a Au nanoring as shown in Fig. 1, was developed to detect a persistent current as reported previously. Firstly, a 20-nm-thick FePt epitaxial film was grown on a MgO(001) substrate by sputtering, which was patterned into nanopillar arrays with the diameter of 100 and 150 nm with combination of electron-beam lithography and Ar-ion milling under the optimised condition. A 30-nm-thick Au film was then deposited onto the sample and patterned into a nanoring with the outer diameter between 355 and 530 nm in the same manner. All the quantum devices were observed by scanning electron microscope (SEM) to confirm a successful configuration as depicted in Fig. 1: the FePt nanopillar stays inside the Au nanoring. Finally, 10 nm Cr/150 nm Au electrical pads for wire-bonding were fabricated onto the devices by photolithography and sputtering. These successful devices were then set in a low-temperature cryostat at 356 mK.

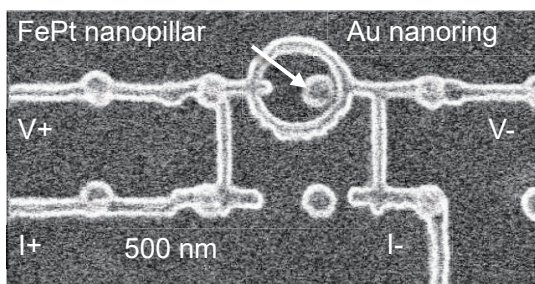


Fig. 1 SEM image of a quantum device.

At 356 mK, a clear hysteresis in magnetoresistance with magnetic field (stray field) reversal in this field range shown in Fig. 2. In our quantum device, an FePt nanopillar with perpendicular anisotropy is expected to produce a stray field with slightly tilted angle from the plane normal onto a Au

nanoring at $H \sim 1$ T, which has theoretically been predicted to induce a persistent current in a nanoring [1]. The persistent current is anticipated to disturb spin-current flow in the nanoring introduced under the non-local measurement geometry, and hence to be estimated by reversing either the direction of the spin-current or that of the stray field. As we reported previously, this is the first experimental demonstration of the persistent current in a metal, which has a potential to offer an alternative way to generate a spin current.

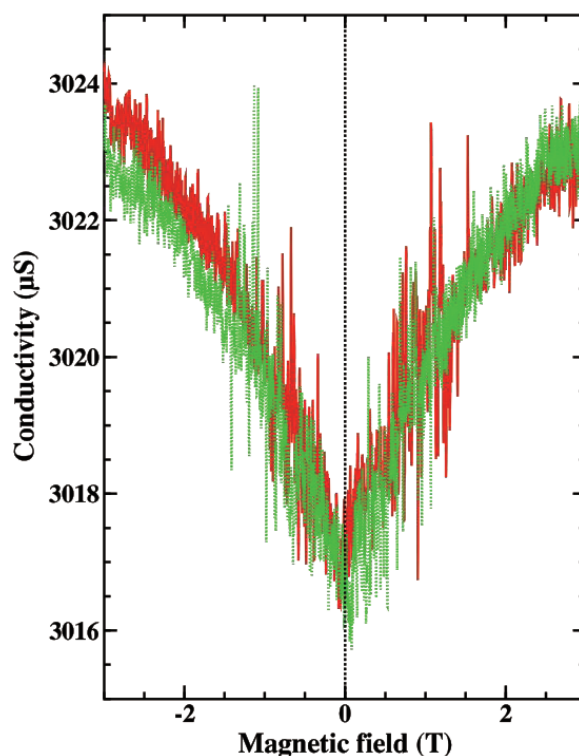


Fig. 1 Magnetoresistance of the quantum device measured under the application of 20 μ V at 356 mK.

References

[1] D. Loss and P. M. Goldbart, *Phys. Rev. B* **45**, 13544 (1992).

Key Words

Spin-polarised persistent current, perpendicular anisotropy, nanoring

Contact to

Atsufumi Hirohata (University of York)

E-mail: ah566@ohm.york.ac.uk

<http://www-users.york.ac.uk/~ah566/>

Advanced High Field X-ray Scattering Studies for Functional Magnetic Materials

An intensive international collaboration has been made to invent the instrumentations for the high magnetic field X-ray scattering experiments. IMR transfer the techniques to generate a compact high magnetic field generator and APS has applied the new strip-line detector for time dependent measurement. The effort has contributed for the improvement of related instrumentations.

The aim of the collaboration is the thorough investigation of magnetic field induced structural effects using a combination of synchrotron x-rays and mini-coil pulsed magnets. Materials under study include frustrated magnets, metamagnets, spin-valves and singlet ground state systems. All of these topical systems enjoy widespread interest in the condensed matter physics community and all will benefit from the use of high-field x-ray diffraction in order to further our understanding. Looking forwards, we would like to proceed beyond diffraction to resonant scattering and to magnetic spectroscopies. These techniques would be very useful to investigate aforementioned functional materials.

The advanced photon source group: Dr. Ruff and Dr. Islam have been collaborating with Nojiri group over the past four years, in an effort to develop new infrastructure and techniques for scattering studies of materials in pulsed magnetic fields. This collaboration will allow for evaluation of previous successes, and for the formation of plans for future collaboration.

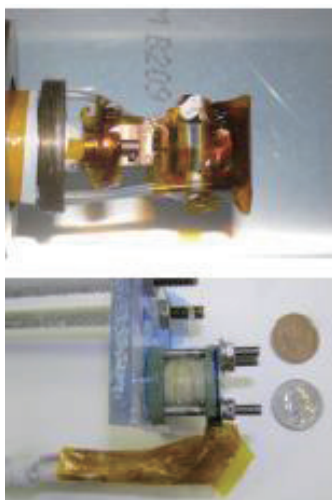


Fig. 1 Mini-split pair coil for X-ray diffraction.

During the visit, we worked at the facilities at Tohoku where mini-coil magnets are prepared, to gain a better understanding of the magnet design side of the ongoing collaborative research effort. Dr. Ruff presented a seminar highlighting recent

successes in the study of frustrated magnetic materials in high field—experiments that were performed at the APS in Chicago using magnet coils of Tohoku design. We made the discussion of new avenues for collaborative exploration, including the identification of condensed matter systems for future study that are of interest to both groups. The highlights of exchanges were discussion on seminal spectroscopic work in pulsed fields and the advanced techniques and time resolved two-dimensional detectors.

Figure 1 shows the photos of the magnet made by the present collaboration. Those are now used heavily at APS for various studies including user program. In the bottom, the coil at the test is shown. The installed form in the tail of a cryostat is in the upper panel. The advantage of this type of coil is in its compactness.

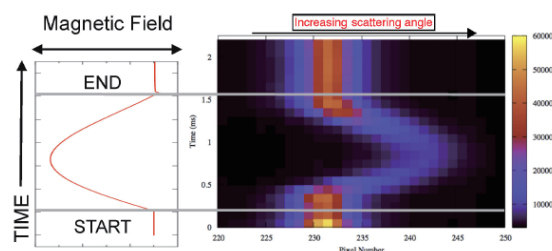


Fig. 2 Time resolved two-dimensional measurement on the field dependence of Bragg peak with a strip line detector.[1]

Figure 2 shows the example of the field dependence of the lattice Bragg peak projected on the high speed-high resolution strip-line area detector. The field dependence of the peak is traced continuously during the pulse. By combining the compact high magnetic field system and the newly developed detector, the efficiency of the experiments has been improved more than one magnitude.

In summary, the present exchange experiences benefited for both sides in the development of technique of high magnetic field X-ray scattering. The output of the collaboration is now working at Advanced Photon Source and is open for world-wide users.

Reference

[1] Z. Islam, submitted to Rev. Sci. Instrum.

Key Words

High Magnetic field, X-ray, instrumentation

Contact to Jacob Ruff (Advance Photon Source, Argonne National Laboratory)

E-mail: jpcruff@aps.anl.gov

Study of Magnetic Phase Diagram of New Triangular Lattice Compound $\text{CsFe}_3(\text{MoO}_4)_2$

Magnetization and electron spin resonance in high magnetic fields have been conducted on a new triangular lattice compound $\text{CsFe}(\text{MoO}_4)_2$. A plateau like structure is found in magnetization at 8 T. The low energy mode of the antiferromagnetic resonance shows the softening at the plateau. The findings indicate the existence of the new phase in magnetic field, which is stabilized by thermal fluctuation.

The frustrated triangular layered systems attract great attention due to complexity of magnetic and ferroelectric structures that appear in them. These structures are due to fierce competition of various exchange interaction within and between layers. Most studied are various compounds ATO_2 with delafossite structure, where $A = \text{Cu, Ag, Na, Li}$, and $T = \text{Fe, V, Cr, Co}$. Recently, new family of layered metal oxides $\text{AT}(\text{MoO}_4)_2$ was studied by means of thermodynamic and resonant techniques as well using the neutron scattering. One member of this family, i.e. $\text{RbFe}(\text{MoO}_4)_2$, possesses Kittel–Yafet 120° structure within layers and experiences a succession of field-induced phase transitions showing pronounced $1/3$ magnetization plateau at low temperatures. Another member of this family, i.e. $\text{KFe}(\text{MoO}_4)_2$, possesses very complicated magnetic structure consisting of alternating 120° triangular layers and helix layers. The goal of proposed research is to study third member of this family, i.e. $\text{CsFe}(\text{MoO}_4)_2$, which property could be intermediated between Rb- and K- based compounds.

The main purpose is the measurements of thermodynamic properties of $\text{CsFe}(\text{MoO}_4)_2$ such as magnetization in high magnetic fields. Analysis of the different phases by resonant technique would be also useful. It is possible that this compound possesses ferroelectric properties in magnetically ordered phase, which also deserves investigation. The establishment of magnetic phase diagram contributes to rich physics of strongly frustrated magnetic systems.

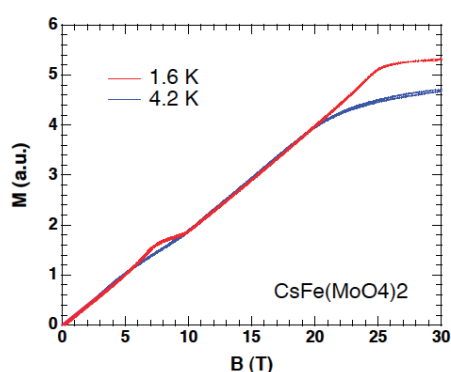


Fig. 1 Magnetization curves at 1.6 K and 4.2 K.

Figure 1 shows the magnetization curves taken at two temperatures, 1.6 K and 4.2 K. At 1.6 K, a plateau structure is found at 8 T. The plateau becomes less clear at 4.2 K. Another feature is the reduction of the magnetization in high magnetic field region at 1.6 K. A plateau in magnetization has been widely found in different triangular based system. The major origin is so called order by disorder. In this mechanism, a plateau is

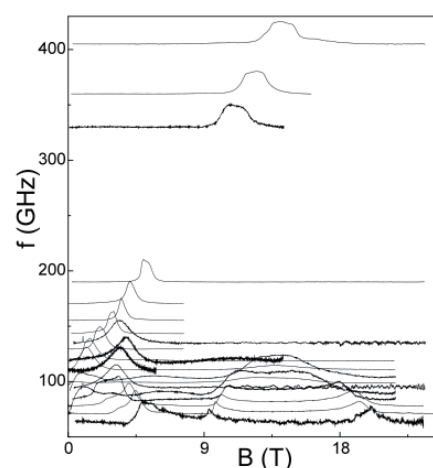


Fig. 2 ESR spectra at 1.6 K. The offset is given so that each position corresponds with the frequency of each spectrum.

stabilized by the lifting of degeneracy by the entropy term, which is originated by quantum or thermal fluctuations. In the present case, the thermal fluctuation must be dominant because the spin is as large as $S=5/2$.

In Fig. 2, ESR spectra are shown. Three low energy modes go to zero frequency. Two of them merge at 8 T. One mode goes down toward the saturation field. The former behavior indicates that the high field and the low field phases become unstable at the plateau phase. Finally, we point out that the non-saturation of magnetization at 25 T suggests that there is a non-collinear phase in high magnetic field, which has a potential to be ferroelectric.

In summary, we found a plateau phase in new triangular lattice compound $\text{CsFe}(\text{MoO}_4)_2$ by means of magnetization and ESR. The completed phase diagram study of the series compounds would contribute the understanding of the magnetic and the electric properties of $\text{AT}(\text{MoO}_4)_2$ family.

Key Words

High Magnetic field, frustration, low-dimensional

Contact to Alexander Vasiliev (Moscow State University)

E-mail: vasil@mig.phys.msu.ru

High-frequency ESR study of the two-leg spin ladder BiCu_2PO_6

We have examined the low energy excitation of the two-leg spin ladder system BiCu_2PO_6 by using the high frequency ESR in IMR. A low-lying excitation develops above the critical field is found when magnetic field is applied along the a -axis. The anisotropy of ESR intensity shows the strong mixing between the singlet ground and the excited states.

Quantum phase transition in antiferromagnets is the subject of current interest. Recently, we have synthesized a ladder compound BiCu_2PO_6 with strong inter-ladder interaction. This compound places close to a quantum critical point between $S=1/2$ two-dimensional antiferromagnet and isolated ladder. Thus, this compound provides a nice opportunity to investigate the intermediate regime between two extreme cases. The elementary excitations of the isolated ladders are triplet excitations. By introducing inter-ladder couplings the triplet excitations will be dressed. Up to now, however, there is no detailed study on the exact nature of the low-energy excitations. Of particular, the moderate values of the spin gap and exchange interactions in BiCu_2PO_6 enable us to explore such magnetic excitations in a wide temperature range, well below and well above the gap temperature. In proximity to a quantum critical point, ESR can serve as an ideal probe for mapping out a spin dynamics as well as for identifying the nature of the low-energy excitations.

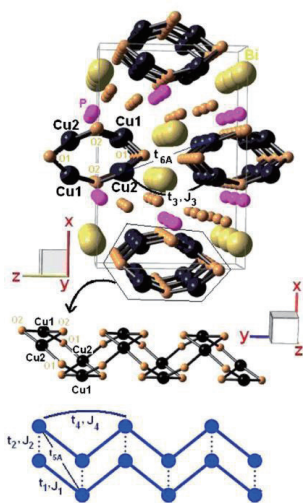


Fig. 1 Crystal structure of BiCu_2PO_6 .

Figure 1 shows the crystal structure of BiCu_2PO_6 (space group $Pnma$). We have synthesized a mm-size single crystal. The static magnetic susceptibility shows a broad maximum around 57 K and then an exponential drop. This is typical for a spin gap system without a long-range magnetic ordering. The

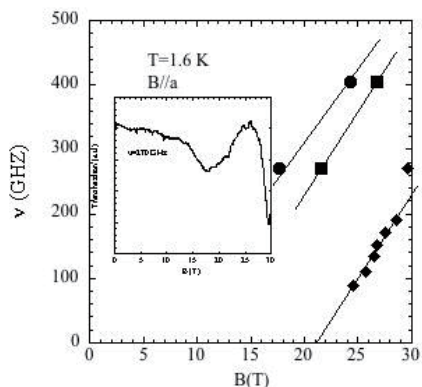


Fig. 2 ESR spectrum at 270 GHz for an external field parallel to an a -axis and the frequency-field plot at 1.6 K

two-leg ladders run along the crystallographic b direction. The spin gap is estimated to be $\Delta \approx 34$ -50 K. The intra-ladder interaction is an order of 80 K and the ratio of the rung hopping to the leg one is $J_{\text{rung}}/J_{\text{leg}} \approx 1$. The inter-ladder coupling of $J_{\text{inter}}/J_{\text{leg}} \approx 0.7$ is substantial. Thus, BiCu_2PO_6 realizes a strongly coupled two-leg ladder.

Figure 2 shows the ESR spectrum for an external field parallel to an a -axis and the frequency-field plot at 1.6 K. We found that one low-lying mode appears at the critical field and grows with increasing magnetic fields. It is the lowest triplet modes which cause the level crossing at the critical field. In higher frequencies, two other modes are also found. The intensities of those modes are very strong and the extrapolations do not intercept the origin of the plot. The latter finding indicates the existence of the internal magnetic field, presumably for the antiferromagnetism. The low-lying mode disappears around 7 K with a small softening of frequency. This temperature corresponds to the ordering temperature of the magnetic field induced antiferromagnetic phase.

In summary, we have investigated the magnetic excitation of the spin ladder compound BiCu_2PO_6 and found the change of the ESR modes in the spin singlet-antiferromagnetic phase boundary.

Key Words

High Magnetic field, quantum critical, spin-ladder

Contact to Kwang-Yong Choi (Department of Physics, Chung-Ang University)

E-mail: kchoi@cau.ac.kr

Solving Large-scale Scientific Problems using Public Resource Computing

Exchange of experience in constructing and handling a public resource computing: PRC has been made between Bielefeld and IMR. The seminar was given to explain the PRC project in Bielefeld called Spinhenge@home. The project provides the scaling computer power in Monte-Carlo type simulations and others on thermodynamic properties of magnetic systems.

The majority of the world's computing power is no longer in supercomputer centers and institutional machine rooms. Instead, it is now distributed in nearly one billion personal computers all over the world. This change is critical to scientists whose research requires extreme computing power. The first so-called "public resource computing" (PRC) project SETI@home has attracted more than two million participants who donate time on their home PCs to a scientific effort. Work is underway to create similar projects in many other areas, enabling scientific explorations that were previously infeasible.

Our PRC project Spinhenge@home is not just one of the largest projects in the world, it is the first and only project that deals with the simulation of complex magnetic structures by means of spin dynamics methods. The image of the home page is introduced in Fig. 1. An example of the calculation made at Spinhenge@home is given in Fig. 2. The implications of the "public resource computing" paradigm are social as well as scientific. It provides a basis for global communities centered around common interests and goals. It creates incentives for the public to learn about current scientific research.

During my stay, we have discussed several common interests and held a seminar about the PRC. In the seminar, an overview of the new and fascinating PRC technology was introduced and its potential was discussed in the context of modern high performance computing challenges for academic and industrial applications.

The discussion included following points.

1. Technology and organization of PRC in Germany
2. Budget and human resource efforts to build up such a center at IMR
3. Applicability of PRC for material science

The exchange of the knowledge and experience with the "Spinhenge@home" project was quite useful for the IMR. A scope of how such a technology can be used by IMR and in Japan in general was discussed in details. At this moment, there is no

such project in Japan, especially in the area of material science.

It is highly

important and is desired to consider such strategy in Japan, especially in the context of the new supercomputer that will be used on the network type computational infrastructure.

Besides PRC, we have discussed about collaboration in the wide range of molecular based magnetic materials, including Keplarate and other clusters showing distinct quantum phenomena. The list of the subjects is given below.

1. Simulation on the multi-core complexes
2. Dipolar order in isotropic molecular magnet array
3. ESR of V_{20} Keplarate based ring

4.

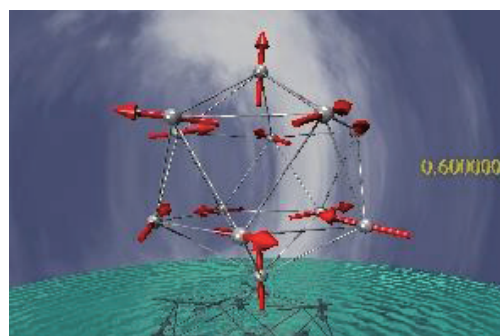


Fig. 2 An example of calculation demonstrated at Spinhenge@home.

Simulation of the large molecule of Fe_9 in high magnetic fields

In summary, the present collaboration was very fruitful for the discussions about the feasibility of PRC in material science and collaboration in the study of molecular magnetism.

Key Words

High Magnetic field, ESR, single crystal

Contact to Christian Schroeder (University of Applied Sciences Bielefeld, Germany)

E-mail: christian.schroeder@fh-bielefeld.de

Fig. 1 The homepage of the Spinhenge@home.

High-magnetic-field Measurements and Single Crystal Growth

Exchange of experience of high magnetic field measurements-ESR and magnetization, and single crystal growth has been made at Nojiri and Yamada groups. Several types of single crystal were grown and characterized by using high magnetic field. The present collaboration was made as single visit and the fellowship programs.

The Wuhan National High Magnetic Field Center at Huazhong University of Science and Technology: HUST is the first high magnetic field research laboratory in China. It has collaborated with the magnetism division of IMR in many different topics. The laboratory is going to introduce advanced equipments developed in IMR, especially those of ESR and low temperature. On the other hand, HUST is offering a technique to build a high magnetic field pulse coil. As such, the collaboration has been successful so far.

The HUST pulsed magnetic field facility is very new. Thus there are lots of things to learn from IMR. The purpose of the present visit is to learn the advanced skills in IMR in following fields through the collaboration researches. During the visit, we have conducted (1) the experiments in high magnetic field, magnetization and ESR at low temperature, (2) the process of single crystal growth, find the effect of parameters of single crystal furnace upon the crystal quality, and eventually made single crystals with our own compounds. It was made at Yamada laboratory.

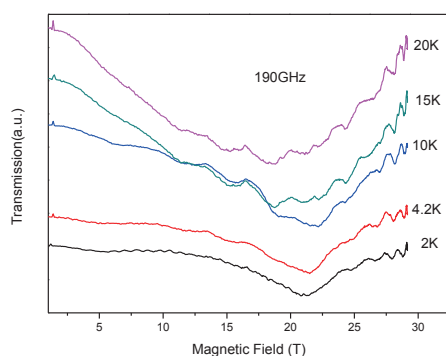


Fig. 1 Temperature dependence of ESR signal of $\text{Ca}_3\text{CoMnO}_6$ at 190 GHz.

Figure 1 shows an example of ESR measurement on Co-oxide crystal. At $T=20$ K, a very broad resonance was found at around 18 T. The full width at half maximum is order of 10 T. When temperature decreases down to 2 K, the center is located at 21 T and the width shrink down to 3 T. The resonance field is much apart from the conventional paramagnetic resonance and thus there must be a strong exchange coupling and the anisotropy. We have measured the frequency dependence of

the spectrum at 2 K and found that the effective g -value is about 1.1. Assuming that the effective g -value is independent of magnetic field, the mode intersects with the zero frequency at around 12 T. This value means that either there is an exchange field of about 12 T or there is a zero field splitting of 350 GHz. The small g -value indicates that there is a sizable zero field splitting. The rapid broadening of the line width at higher temperature is attributed to the fast relaxation caused by the strong contribution of the orbital moment. The small g -value is



Fig. 2 $\text{La}_{1.67}\text{Sr}_{0.33}\text{NiO}_4$ single crystal

consistent with such orbital contribution.

Figure 2 shows the single crystal grown during the visit. The growth was made by using the floating zone machine at Yamada laboratory. We could confirm the orientation and the quality by using X-ray photograph. The important techniques for single crystal growth have been exchanged during the stay. It would contribute to the single crystal section at the high magnetic field laboratory of HUST.

In summary, the present exchange visit had a large merit to learn the advanced techniques of IMR in high magnetic field experiments and in single crystal growth. In the side of IMR, the various new compounds from China will be examined by this collaboration. Such collaboration will contribute to the formation of high magnetic field research network in east-Asia region and push up the status of both laboratories in the international community of high magnetic field research.

Key Words

High Magnetic field, ESR, single crystal

Contact to Zhongwen Ouyang (Wuhan National High Magnetic Field Center HUST)

E-mail: zwouyang@mail.hust.edu.cn

First-principles and molecular-dynamics simulations of ferroelectrics

We are developing our original molecular-dynamics simulation code for ferroelectrics based on the effective Hamiltonian constructed from first-principles calculations. Currently, the code can simulate finite-temperature properties of BaTiO_3 , KNbO_3 and PbTiO_3 . Not only bulk properties but also properties of thin-film capacitors can be simulated.

1 Introduction

We are developing our original molecular-dynamics (MD) simulation code[1] for ferroelectrics based on the effective Hamiltonian constructed from first-principles calculations[2, 3, 4]. It is named “feram” and distributed as free software from <http://loto.sourceforge.net/feram/>. We have already constructed a set of parameters of the effective Hamiltonian for BaTiO_3 [5].

This year, 2010, we newly constructed sets of parameters of effective Hamiltonians for KNbO_3 . We also constructed a set of parameters of effective Hamiltonian for PbTiO_3 by translating previous notation of its effective Hamiltonian[4] into new one.

2 KNbO_3

KNbO_3 is one of the candidates of lead-free (Pb-free) ferroelectrics. Knowing and simulating finite-temperature dynamical properties such as phase transitions, polarization switching and so on are important. Using the parametrization method described in Ref.[5] and Wu and Cohen’s recently developed generalized-gradient approximation (GGA) functional[6], we newly constructed a set of parameters of effective Hamiltonian for this ferroelectric material. As a result of MD simulation, in Fig. 1, temperature dependence of lattice constants are shown. Three phase transitions, cubic-tetragonal-orthorhombic-rhombohedral, are clearly simulated with hysteresis in temperature, cooling-down and heating-up.

3 PbTiO_3

PbTiO_3 is one of the fundamental ferroelectric materials as a component of solid solution such as $\text{Pb}(\text{Zr}, \text{Ti})\text{O}_3$, $\text{PbMg}_{1/3}\text{Nb}_{2/3}\text{O}_3$ - PbTiO_3 and so on. For developing Pb-free ferroelectrics, knowing and simulating finite-temperature properties of PbTiO_3 itself is

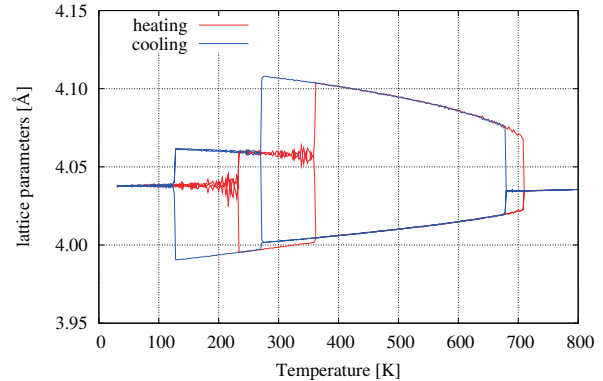


Figure 1: Simulated temperature dependence of lattice parameters of KNbO_3 .

also important. We constructed a set of parameters of effective Hamiltonian for PbTiO_3 by translating previous notation of its effective Hamiltonian[4] into the current version.

It is known that 90° domain structures are sometimes observed in bulk and thick films of PbTiO_3 [7]. In a cooling-down simulation of bulk PbTiO_3 , as shown in Fig. 2, 90° domain structure is successfully reproduced.

4 Future plan

Currently, as described above, we are constructing sets of parameters of effective Hamiltonians for wide range of perovskite-type ferroelectrics. We are improving **feram** code for simulating ferroelectric solid solutions such as $\text{Pb}(\text{Zr}_x\text{Ti}_{1-x})\text{O}_3$ (PZT), $\text{Pb}(\text{Sc}_{1/2}\text{Nb}_{1/2})\text{O}_3$ (PSN) and $\text{Pb}(\text{Mg}_{1/3}\text{Nb}_{2/3})\text{O}_3$ (PNM). We are also improving computational speeds of simulations by optimization and parallelization of the code.

We believe that our **feram** code can be a powerful tool for simulating and understanding fundamental physics of ferroelectrics. Moreover, because it can simulate not only bulk properties but also properties of thin-film capacitors, it will be also used for developing and improving applications of ferroelectrics such as multilayer ceramic capacitors (MLCC), non-volatile ferroelectric memories (FeRAM), etc.

We are also implementing capability of non-equilibrium simulations to **feram** code. In the very near future, we can use the code to estimate thermal conductivity of ferroelectrics, which is relevant to electro-caloric applications. Molecular-dynamics simulation of ferroelectric domain-wall pinning by de-

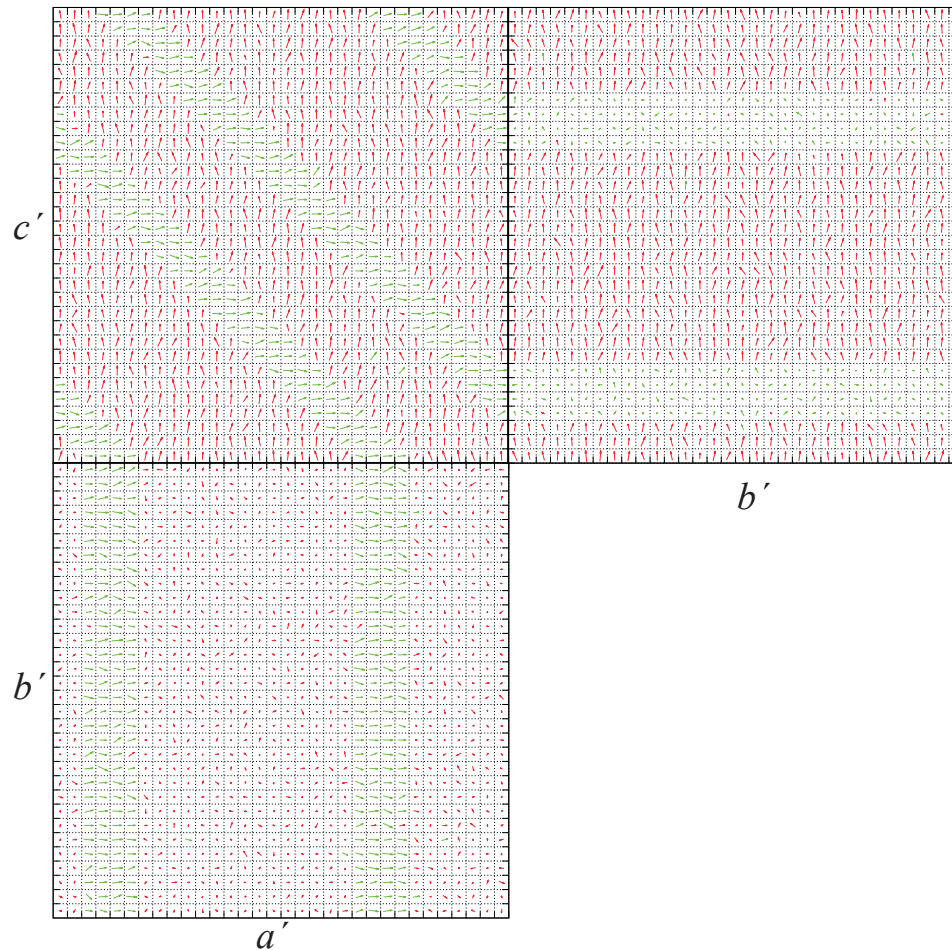


Figure 2: Snapshot of three “sides” of the $32 \times 32 \times 32$ supercell at $T = 300\text{K}$ in a cooling-down simulation of PbTiO_3 . Dipole moments of each site are projected onto the planes and indicated with arrows. Dipoles of $u_z > 0.2\text{\AA}$ are indicated with red color. Dipoles of $u_z \leq 0.2\text{\AA}$ are indicated with green. Crystalline directions are indicated with a' , b' , and c' .

fects during switching of polarization is also one of our targets of non-equilibrium simulations.

References

- [1] T. Nishimatsu, U. V. Waghmare, Y. Kawazoe and D. Vanderbilt, Phys. Rev. B **78**, 104104 (2008).
- [2] R. D. King-Smith and D. Vanderbilt, Phys. Rev. B **49**, 5828 (1994).
- [3] W. Zhong, D. Vanderbilt and K. M. Rabe, Phys. Rev. B **52**, 6301 (1995).
- [4] U. V. Waghmare and K. M. Rabe, Phys. Rev. B **55**, 6161 (1997).
- [5] T. Nishimatsu, M. Iwamoto, Y. Kawazoe and U. V. Waghmare, Phys. Rev. B **82**, 134106 (2010).
- [6] Z. G. Wu and R. E. Cohen, Phys. Rev. B **73**, 235116 (2006).
- [7] K. Aoyagi, T. Kiguchi, Y. Ehara, T. Yamada, H. Funakubo and T. J. Konno, Sci. Technol. Adv. Mater. **12**, 034403 (2011).

Keywords

first-principles calculation, molecular dynamics, simulation, ferroelectrics, FeRAM

Contact to

Takeshi Nishimatsu

Institute for Materials Research (IMR),
Tohoku University, Sendai 980-8577, Japan
Email: t-nissie@imr.tohoku.ac.jp
<http://t-nissie.users.sourceforge.net/>

Umesh V. Waghmare

Theoretical Sciences Unit, Jawaharlal Nehru Centre
for Advanced Scientific Research (JNCASR), Jakkur,
Bangalore, 560 064, India
Email: waghmare@jncasr.ac.in
<http://www.jncasr.ac.in/waghmare/>

Study of spin correlations in geometrically frustrated systems using polarized neutron and pulsed magnetic fields

Masaaki Matsuda

Neutron Scattering Science Division, Oak Ridge National Laboratory, Oak Ridge, TN 37831, USA

By the support of ICC-IMR Program, I visited IMR from January 5th to 8th, 2011, and discussed a project of neutron diffraction experiments of geometrically frustrated spin systems by polarized neutron and high pulsed magnetic fields with collaborators, in particular, in Yamada Lab. and Nojiri Lab, which have the world top level technology of high field neutron diffraction experiments.

When one applies a high external magnetic field to spin systems, novel phenomena sometimes arise. A typical one is fractional plateaus in magnetization (M-H) measurements in geometrically frustrated spin system, in which the regular triangular arrangement of spins induces degenerate ground state. For a tetrahedron that consists of four isotropic classical spins, any spin configuration with a null total spin can be the ground state; thus, infinite number of spin states satisfies the criterion under this situation. When a corner-sharing 3D network with such a tetrahedron lattice, which is called the pyrochlore lattice, is arranged, degeneracy of the ground state becomes macroscopic. The Cr-based spinels ACr_2O_4 (A=Hg, Cd, and Zn) are typical ones of the pyrochlore lattice [1]; ACr_2O_4 has a cubic Fd-3m structure in which the magnetic trivalent Cr ions without orbital degeneracy form the pyrochlore lattice (Fig.1). The macroscopic degeneracy in the pyrochlore system induces exotic magnetic properties at low temperatures.

To investigate the induced magnetic transitions based on spin frustration, clarification of the change of spin arrangements is indispensable. The most effective probe for the investigation is the neutron diffraction technique under high magnetic fields. Since typical transitions in the frustrated spin systems occur

above a few 10 Tesla, 40 T class magnetic field experiments are required. Moreover, for spin systems with high crystallographic symmetry, polarized neutrons are quite important to determine accurate spin directions. Since IMR exclusively has world top technology in this field, discussions in IMR were indispensable for investigations in the frustrated spin systems.

During the stay in IMR, a detail of the project of neutron diffraction experiments of geometrically frustrated spin systems in high pulsed magnetic fields was discussed with collaborators in Nojiri Lab. of IMR. In this project, we are aiming at installing a pulsed magnetic field system for neutron diffraction to SNS and HIFR of Oak Ridge National Laboratory (ORNL). We discussed its feasibility and technical problems of the experiments, in particular a condenser bank that will be installed to ORNL. Moreover, we determined the role of each collaborator in the investigations of geometrically frustrated spin systems. By the discussion, we have reached an agreement on operation of high magnetic field experiments in ORNL.

Since Tohoku Univ. is advancing a project to construct a polarization analysis neutron spectrometer in J-PARC, based on a collaborative project with KEK, and the Yamada Lab. is the center of the project, roles of polarized neutron technique in this field were discussed with collaborators in Yamada Lab. A meeting with collaborators in KEK, JAEA, and J-PARC was held as well. In the discussion, I explained the key investigations of this field by polarized neutron, and proposed future ambitious roles of this technique.

References

[1] M. Matsuda, K. Ohoyama, S. Yoshii, H. Nojiri, P. Frings, F. Duc, B. Vignolle, G. L. J. A. Rikken, L.-P. Regnault, S.-H. Lee, H. Ueda, and Y. Ueda Phys. Rev. Lett. 104, 047201 (2010).

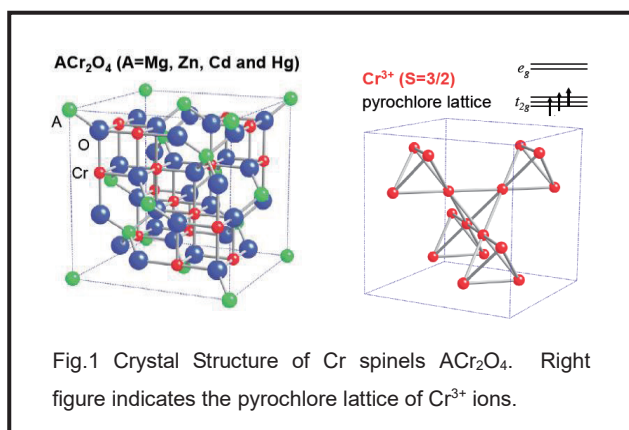
Key Words

Spin frustrated systems, neutron diffraction, pulsed magnetic fields, polarized neutron

Contact to

Kenji Ohoyama (Yamada Lab.)

E-mail: ohoyama@imr.tohoku.ac.jp



Theory of spin Seebeck effect --- Gerrit E.W. Bauer

This is a report about Bauer's visit to the IMR in the first week of February 2011. Discussions were carried out on the physics of the spin Seebeck effect in various systems. Strategies to increase the thermoelectric figure of merit were assessed.

The spin Seebeck effect discovered by Uchida, Saitoh and coworkers [1-3] opens new possibilities to generate useful power out of waste heat. The configuration discussed theoretically is plotted in Fig. 1 [4]. In order to become really useful, it is of utmost importance to increase the thermoelectric figure of merit.

During the stay at the IMR Bauer discussed the physics of the spin Seebeck effect and related phenomena with the experimentalists at the IMR in the Saitoh and Takanashi groups with emphasis on the efficiency of the first generation of experiments on magnetic insulator electronics. If the effects are to be useful, they must be significantly enhanced. This can be done by material science, modifying the doping and chemical composition of the insulators in order to increase magnetization and spin wave stiffness, without increasing the damping. The detection efficiency by the inverse spin Hall effect can possibly increase by finding a metal with very large spin Hall angles, or interface engineering.

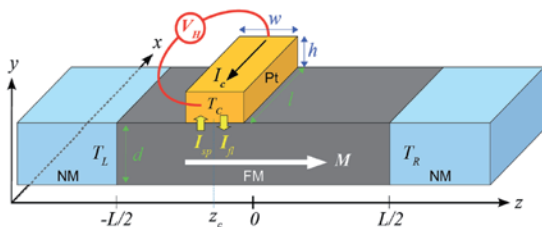


Fig. 1: Geometry of the spin Seebeck effect. A temperature difference $T_R - T_L$ over the ferromagnet (FM) leads to a heat current parallel to the magnetization M . The inverse spin Hall effect then induces a transverse current I_c or voltage V_H .

We wish to integrate the theories for contacts to and spin wave propagation in the magnetic insulator Yttrium Iron Garnet (YIG) in order to understand simple and complex circuits and devices. This comes down to a generalization of an earlier developed magnetoelectronic and magnetocaloritronics circuit theory. To this end it is important to discuss possible future devices and architectures with experimentalists.

Our theoretical formalism [4] will allow us to reappraise the thermoelectric properties and heat engines based on magnetic insulators. We expect that the very small damping will be very favorable for the energy conversion efficiency.

Another strategy is the search for material combinations that employ a large mixing conductance. To this end we studied the band structure of YIG and the mixing conductance with a normal

metal in collaboration with the group of Ke Xia at Beijing Normal University [5]. As a result we found that the mixing conductance with YIG can be of the order of that of a good intermetallic

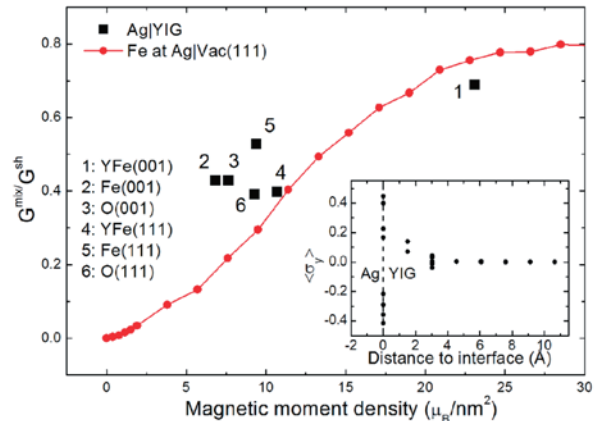


Fig. 2: Spin mixing conductance of the Ag|YIG interface for different interface cuts and directions (filled squares) in units of the Ag Sharvin conductance as a function of the interface magnetic moment density. The red curve is the mixing conductance of the Ag|Vacuum interfaces with a varying number of Fe moments distributed randomly over the surface [5].

contact, presumably due to the strong interaction of the conduction electrons in the metal with the local iron moments of the ferromagnetic insulator (see Fig. 2). These results open the exciting possibility that the figure of merit of the spin Seebeck effect for YIG can be increased by two orders of magnitude.

References

- [1] K. Uchida, S. Takahashi, K. Harii, J. Ieda, W. Koshibae, K. Ando, S. Maekawa, and E. Saitoh, *Nature* **455**, 778 (2008).
- [2] K. Uchida, J. Xiao, H. Adachi, J. Ohe, S. Takahashi, J. Ieda, T. Ota, Y. Kajiwara, H. Umezawa, H. Kawai, G.E.W. Bauer, S. Maekawa and E. Saitoh, *Nature Mater.* **9**, 894 (2010).
- [3] S. Bosu, Y. Sakuraba, K. Uchida, K. Saito, T. Ota, E. Saitoh, K. Takanashi, *Phys. Rev. B* **83**, 224401 (2011).
- [4] J. Xiao, G.E.W. Bauer, K. Uchida, E. Saitoh, and S. Maekawa, *Phys. Rev. B* **81**, 214418 (2010).
- [5] X. Jia, K. Liu, K. Xia, G.E.W. Bauer, arXiv:1103.3764.

Key Words

Spin Seebeck effect, spin caloritronics, YIG.

Contact to

Gerrit E.W. Bauer

E-mail: g.e.w.bauer@tudelft.nl

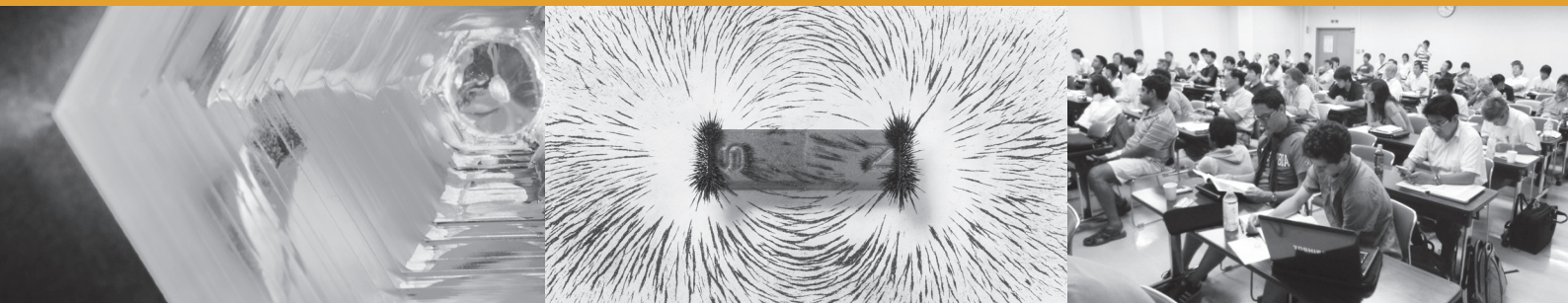
<http://sites.google.com/site/gewbauer/>

ICC-IMR FY2010 Activity Report

Edited by ICC-IMR Office
Published in February, 2018

Contact: International Collaboration Center,
Institute for Materials Research (ICC-IMR)
Tohoku University
2-1-1, Aoba-ku, Sendai, 980-8577, Japan
TEL&FAX: 81-22-215-2019
E-mail: icc-imr@imr.tohoku.ac.jp

Printing: HOKUTO Corporation



この冊子は「水なし印刷」
により印刷しております。



環境にやさしい植物油インク
[VEGETABLE OIL INK]で
印刷しております。